Submonthly Assessment of Temperate Forest Clear-Cuts in Mainland France

Stéphane Mermoz, Juan Doblas Prieto, Milena Planells, David Morin, Thierry Koleck, Florian Mouret, Alexandre Bouvet, Thuy Le Toan, David Sheeren, Yousra Hamrouni, Thierry Bélouard, Éric Paillassa, Marion Carme, Michel Chartier, Simon Martel, and Jean-Baptiste Féret

***Abstract*—Remote sensing satellites allow large-scale and fast detections of forest loss. Operational forest loss detection systems have been mainly developed over tropical forests; however, it is increasingly important to have access to accurate and up-to-date information on temperate forests. In this article, we adapted a Sentinel-1-based near real-time tropical forest loss detection method, based on the radar change ratio, to detect French temperate forests clear-cuts. Using ancillary data, annual and submonthly clear-cuts were assessed for broadleaf and conifer forests, for various tree species, over public and private forests. Using 967 validation plots, the maps exhibited recall and precision of 80.9% and 99.4%, respectively. The clear-cuts area shows remarkable stability over time from 2020. We found seven times more clear-cuts in private forests than in public forests, although the surface area of private forests is only three times that of public forests. It was also demonstrated that only 1.6% out of 4 530 dieback reference plots, and 6.2% of maps of forest bark beetle attacks, were confused with clear-cuts before clear-cuts actually occurred, which makes our maps complementary with forest dieback maps. Collectively, the findings of this study could have significant implications for the implementation of a radar-satellite-based system designed for the real-time detection of large-scale clear-cuts in European temperate forests.**

***Index Terms*—Fast clear-cuts detection, France, Sentinel-1 SAR image time series, temperate forests.**

Manuscript received 11 January 2024; revised 3 April 2024 and 2 June 2024; accepted 30 June 2024. Date of publication 18 July 2024; date of current version 9 August 2024. This work was supported in part by ADEME through the SuFoSaT (French forests monitoring from satellites) project under Grant 2003C0077, through the GRAINE programme, in part by the CNES, and in part by the Ministry of Europe and French Forest Affairs through the TropiSCO project of the Space Climate Observatory under Grant 230887/00. *(Corresponding author: Stéphane Mermoz.)*

Stéphane Mermoz and Juan Doblas Prieto are with GlobEO, 31400 Toulouse, France (e-mail: mermoz@globeo.net).

Milena Planells, David Morin, Thierry Koleck, and Alexandre Bouvet are with CESBIO, CNES/CNRS/INRAE/IRD/UPS, Université de Toulouse, 31400 Toulouse, France.

Florian Mouret is with the USC INRAE 1328/P2E laboratory (Physiology, Ecology and Environment), Université of Orléans, 45067 Orléans, France, and also with the CESBIO, CNES/CNRS/INRAE/IRD/UPS, Université de Toulouse, 31401 Toulouse, France.

Thuy Le Toan is with GlobEO, 31400 Toulouse, France, and also with the CESBIO, CNES/CNRS/INRAE/IRD/UPS, Université de Toulouse, 31400 Toulouse, France.

David Sheeren is with the Département Sciences de l'Ingénieur et du Numérique, UMR 1201 DYNAFOR INRAE/INP-ENSAT/INP-EI Purpan, ENSAT, 31326 Auzeville-Tolosane, France.

Yousra Hamrouni is with the INRAE, UMR DYNAFOR, Castanet-Tolosan, Université de Toulouse, 31400 Toulouse, France.

Thierry Bélouard is with the Département santé des Bélouard, UMR1202 BIOGECO, Centre INRAE Nouvelle Aquitaine, 33610 Cestas, France.

Éric Paillassa is with the CNPF-IDF, Antenne de Bordeaux, 33075 Bordeaux, France.

Marion Carme is with the INRAE UMR 1202 BIOGECO, Université de Bordeaux, 33615 Pessac, France.

Michel Chartier is with CNPF-IDF, 45023 Orléans Cedex, France.

Simon Martel is with the CNPF-IDF, Antenne de Bordeaux, 33075 Bordeaux, France.

Jean-Baptiste Féret is with the TETIS, AgroParisTech, Cirad, CNRS, INRAE, Université de Montpellier, 34090 Montpellier, France.

Data is available online at: https://ee-sufosatclearcuts.projects.earthengine.app/view/sufosat-clearcuts.

Digital Object Identifier 10.1109/JSTARS.2024.3429012

I. Introduction

THE Earth's forests serve as crucial repositories of biodiversity and substantial carbon reservoirs that help regulate the climate. In fact, forests act as a carbon sink by capturing carbon from the atmosphere through tree growth, and as a carbon source through deforestation and forest degradation although part of the carbon remains stored in the wood products. The deterioration of these forests also significantly contributes to the decline of biodiversity due to habitat destruction, soil erosion, disruptions in the terrestrial water cycle, and human-induced CO_2 emissions.

Earth Observation allows large-scale and fast detection of forest loss. Various satellite-based forest loss detection systems have already been developed. Examples include forest monitoring for action [1], Terra-I [2], and Institute for Hydrology, Meteorology and Environmental Studies (IDEAM) systems, which were designed for both national (IDEAM) and pantropical scales. These systems are based on acquisitions from the moderate resolution imaging spectroradiometer (MODIS), providing biweekly, monthly, and quarterly detections at a 250 m spatial resolution. In addition, the Brazilian Real-Time Deforestation Detection DETER-B [3] offers detections at a spatial resolution of 60 m every five days. Furthermore, the Peruvian Ministry of Environment system in Peru issues weekly forest alerts through the Peruvian National Forest Conservation Program early warning alerts, while the Global Land Analysis and Discovery (GLAD) team at the University of Maryland (UMD) produces global and annual forest loss [4] and tropical and weekly forest alerts [5], with both systems relying on Landsat data at a 30 m resolution. All these systems are based on optical and multispectral images. SAR-based detection systems, mostly based on Sentinel-1 data, have also been developed recently because SAR imagery holds immense promise due to

TABLE I
DATA USED IN THE STUDY

Data	Time Span	Spatial Res./Qty.	Description	Source	Reference	Usage
Radar backscattering	2020–2023	10 m	Sentinel-1 C-band SAR data	Copernicus	-	clear-cuts detection
Forest loss	2020–2022	30 m	Annual tree cover loss maps from Landsat at the global scale	Global Forest Watch	[4]	Comparison
Clear-cuts	2020–2023	30 m	Annual clear-cuts maps from Sentinel-2 at the national scale	French Ministry of Agriculture, INRAE (under request)	[17]	Comparison
Forest loss	2020–2022	30 m	Annual tree cover loss maps from Landsat at the European scale	Zenodo	[29]	Comparison
Bark beetle attacks	2020–2022	10 m	Spruce mortality following bark beetle outbreaks detected from FORDEAD applied to Sentinel-2 time series.	Gitlab	-	Comparison
Snow-covered area	2019–2022	500 m	MODIS/Terra snow cover daily	MODIS MOD10A1	-	Warning masking
Burnt area	2019–2022	30 m	EFFIS burnt area polygons	EFFIS	-	Warning masking
Dominant leaf type	2018	10 m	Classification providing nonforest areas, broadleaved and coniferous forest	Copernicus LMS	-	Analysis over broadleaf and conifer forests
Tree cover	2018	10 m	Proportional crown coverage per pixel, ranging from 0 to 100%	Copernicus LMS	-	Forest and non-forest mask production and clear-cuts characteristics assessment
Height	2020	10 m	French height map based on Sentinel-1, Sentinel-2, ALOS2, and GEDI data	Zenodo	[34]	clear-cuts characteristics assessment
Forest cover change	2019–2022	967	Reference data obtained from Google Earth VHR images	This study	-	Validation
Dieback	2020–2022	4530	Reference data of declining forests with various levels of diebacks	ONF, DSF and INRAE (Under request)	-	Validation

its partial insensitivity to cloud cover [6]. For notable examples, operational systems such as the forest area change detection system from the Japan Aerospace Exploration Agency [7], [8] based on Advanced Land Observing Satellite-2 (ALOS2) data, radar alerts for deforestation detection [9], TropiSCO from the Space Climate Observatory [10], and real-time deforestation detection—radar [11] based on Sentinel-1 data have been deployed recently thanks to the open access availability of the images. These operational systems have been detailed, validated and compared in [12]. New methods have also been created to detect selective logging [13], [14] and forest loss drivers [15]. It is interesting to note that these operational systems have been created mainly for tropical forest monitoring. Some methods have been tested in temperate and boreal regions [16], [17], [18], [19], but not applied in an operational manner except in Canada [20].

However, temperate forests such as European forests play a key role in preserving and restoring biodiversity and developing the bioeconomy. Moreover, temperate forests are increasingly under threat both from biotic and abiotic disturbances, with the six highly relevant threats being, phenology shifts, wildfires, pest infestations, droughts, storm damages, and illegal logging. Unfortunately, illegal logging soars in Europe, and the frequency and intensity of disturbances are believed to further increase in the near future as a result of the ongoing climate change.

Meanwhile, the demand for biomass is increasing worldwide. In the European Union (EU), the overall use of woody biomass increased by approximately 20% since 2000. In addition to anthropic and natural disturbances, political, social, or economic factors can lead to a modification of management practices, for example, to satisfy an increasing wood demand. The EU application of the "energy from renewable sources" directive and the bioeconomy strategy (started in 2012) are setting increasing wood demand for bio-energy needs, with an established target of at least 32% renewable energy by the year 2030. In parallel, construction is booming in the United States of America, driven by government subsidies, even as taxes are being imposed on Canadian lumber, an essential source of supply. In China, wood consumption has been on the rise for the past decade. After overexploiting its forests, the Chinese government banned oak harvesting on its territory for 99 years, and Russia gradually reduced softwood exports from Siberian forests, before Europe's economic sanctions against Russia linked to the situation in Ukraine. This international context drastically increases pressure on European forests. There is, thus, a need to reconcile this increased demand for wood with sustainable management, including protection and restoration of the forest ecosystems that are producing it.

Nevertheless, there is limited information available regarding the current status of forests in the EU. The status of European forests is assessed based on field plots and sampling, without any consistent wall-to-wall monitoring system available. It is thus increasingly important to have access to accurate, extensive, and up-to-date information on European forests. For example, the European Commission developed an EU-wide forest observation framework (forest monitoring information system for Europe—FISE) to provide open access to detailed, accurate, and timely information on the condition and management of EU forests, using satellite data to a large extent. This information allows improving forest monitoring, reducing illegal logging, and supporting the adaptation of forests to climate change.

In that context, the French forest is of particular importance. It is the fourth most forested country in Europe with 17 million ha and it has experienced an increase of 30% in harvested forest area in 2016–2018 compared to 2004–2015 [21], although this figure is probably overestimated in the French case according to [22]. Legal methods used to renew stands in France, in particular clear cutting, are being the subject of heated debate and unprecedented social mobilization.

Currently, France has one optical-based system for recording yearly forest clear-cuts at the national level, which is not publicly available though [17]. The other current consistent source of information available at the national level is the national forest inventory (NFI) statistical survey that is, however, fully updated every 10 years only by the French national mapping agency (IGN).

In this study, we produced maps of clear-cuts in near real-time over France using Sentinel-1 data, by adapting the method from [23] initially designed for the tropics. These maps, opened to everyone, aim at feeding the French forest observatory to establish forestry policies and carry out effective forest monitoring. These maps are reproducible to the rest of Europe to potentially feed a European forest observatory in near real-time. Using ancillary data, we validated the maps, assessed annual and submonthly clear-cuts for broadleaf and conifer forests, for various species, over public and private forests. The height and tree cover density (TCD) distribution of the forest before being cut were investigated. We also analyzed the temporal evolution of the size of clear-cuts areas. Last but not least, we quantified the confusions between detected clear-cuts and dieback forests using an extensive dieback reference dataset and maps of bark beetle attacks.

Note that in this article, the term "clear-cuts" is defined as a single cut involving the entire or a substantial part of the stand, preceding its regeneration, as in [24]. In fact, natural or artificial regeneration is a legal requirement in France.

The rest of the article is organized as follows. Section II introduces the study site, data, and method used in this study. Results are detailed in Section III and discussed in Section IV. Finally, Section V concludes this article.

II. Material and Method

A. Study Site

The French forest surface area, shown in green in Fig. 1, covers 17 million ha, of which at least 2 million ha planted [25]. With 190 tree species, the French forest contains almost 75% of the tree species found in Europe. In total, 64% of the French forest is made up of broadleaved trees, 44% of which are oaks. Among the most widely planted species, maritime pine is the most common conifer species as the main species and in pure stands (775 000 ha), followed by Douglas fir, spruce, and other conifers. Poplar is the most planted broadleaf tree with 180 000

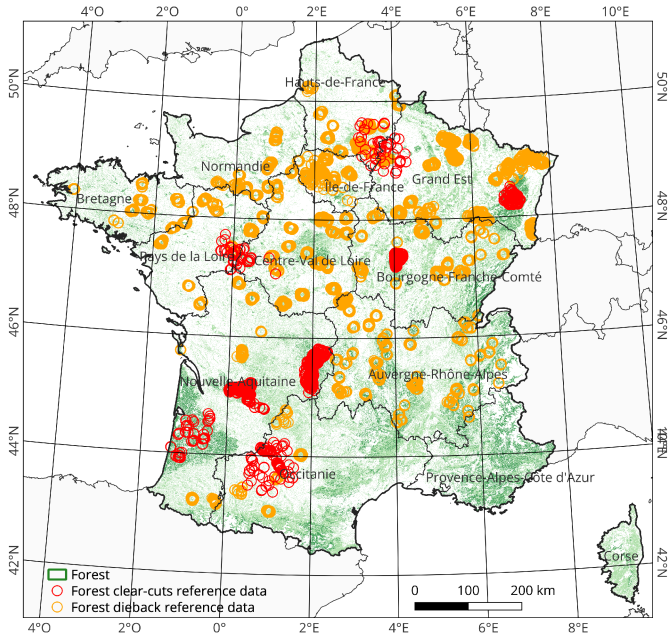

Fig. 1. Study site and reference data.

ha. Mixed plantations with two or more species represent more than 15% of French planted forests [26].

B. Data

The data used in this study are summarized in Table I. Below is a brief description of these different types of data, including reference data, Earth observation data, and higher level products derived from these observations.

1) Sentinel-1 Satellite Data: The clear-cuts detection system is mainly based on Sentinel-1 data, which were processed using the S1tiling toolbox [27] available on Github. We processed only Sentinel-1A and no Sentinel-1B images primarily due to the large amount of Sentinel-1 images over Europe, but also to ensure a homogeneous temporal distribution. In fact, Sentinel-1B experienced an anomaly from December 2021 and the mission ended officially in August 2022. Ground-range detected interferometric wide swath VH-polarized Sentinel-1A images acquired in descending and ascending orbits were calibrated, orthorectified, and filtered using the multitemporal filter described in [28], with a 3×3 window. The filtering kernel (i.e., the mean ratio between spatially filtered images and original images) was calculated using the Sentinel-1 images acquired in 2018 and used to filter each image acquired after January 1, 2019. In order to preserve spatial resolution, no further speckle reduction methods, such as spatial filters, were used. The entire Sentinel-1A archive over this area of interest was processed and clipped along 87 tiles, generating a total number of 100 947 images.

2) Reference Data Used to Validate Clear-Cut Detections: The 967 reference polygons used for validation were manually defined using very high-resolution images made available by the French national facility for institutional procurement of satellite imagery (DINAMIS), Google Inc., and high-resolution Sentinel-2 images, over broadleaf (48% of the reference polygons) and coniferous (52%) forests. In total, 63% of the polygons belong to the "clear-cuts" class, whereas 37% suffered no visible canopy change over the time span of the study ("no clear-cuts" class). The spatial distribution of the polygons is shown in Fig. 1.

3) Competitive Methods: The Global Forest Watch (GFW) tree cover loss map [4] is used here for comparison. It is an annual map of forest cover loss produced by the UMD using Landsat data at a 30 m resolution. The map shows the total deforestation area in a year. For comparison purposes, we also got the clear-cuts map from INRAE [17], under request, over the Landes region from 2020 to 2023. The INRAE detection system described uses the normalized difference vegetation index (NDVI) derived from satellite optical images (SPOT, Landsat, etc.) to detect and map clear-cuts in forests on a yearly basis, with a minimum mapping unit of 1 ha. We also used the annual forest loss map from Technical University of Munich (TUM) [29] for the year 2020, derived from Landsat at the European scale, with a minimum mapping unit of 0.18 ha. Note that our SAR-based clear-cuts detection system was compared with optical-based forest loss or clear-cuts detection system, and both systems do not necessarily detect the same phenomena. While SAR waves penetrating through the clouds are mainly sensitive to soil and vegetation moisture and canopy structure, optical data picture the top-of-canopy and are useful for calculating vegetation indices, such as NDVI, which helps in assessing plant health for example. To summarize, optical and SAR satellite data are two distinct types of remote sensing technologies, each having its unique characteristics, advantages, and limitations.

4) Forest Dieback Reference Data: In our analysis, we investigated the influence of forest dieback on our detection system. We aimed to ensure that dieback forests, characterized by reduced vigor and crown loss but still alive, are not misclassified as clear-cuts. According to the French Forest Health Service, a stand is considered in dieback if more than 20% of its trees have more than 50% canopy loss, i.e., dead branches and missing ramifications in its canopy. To quantify misclassifications of dieback forests as clear-cuts, we leveraged 4 530 forest plots of 20 trees each according to the DEPERIS protocol, labeled across France in various campaigns (see Table II for more details on the analyzed tree species and associated plot numbers). Crucially, these plots represent areas free from clear-cuts, ensuring they should not be flagged by our system. These reference plots have been used to calibrate a dieback detection chain, called RECONFORT, operational for oak, pine, and chestnut in the region of Centre Val de Loire. It is based on two spectral indices extracted from Sentinel-2 visible and infrared bands, related to the chlorophyll and water content in the vegetation. You may refer to [30] for more information on evaluating forest dieback in the case of oak trees, and this website[1] for information related to the DEPERIS method used here for forest health assessment. Note that this forest dieback reference data reflects dieback in general, for example, due to droughts and pests. In the following,

[1][Online]. Available: https://agriculture.gouv.fr/la-methode-deperis-comment-quantifier-et-mesurer-letat-de-sante-dune-foret-et-son-evolution

TABLE II
NUMBER OF REFERENCE DIEBACK PLOTS THAT ARE NOT CUT YET, WHICH WERE DETECTED AS CLEAR-CUTS

	Dieback plots	Dieback plots detected as clearcuts	% of dieback plots detected as clearcuts	% of dieback detected area vs. total area
Oak	2986	10	0,3%	0,1%
Beech	702	38	5,4%	0,8%
Fir	457	10	2,2%	0,3%
Chestnut, 2020	197	0	0%	0%
Chestnut, 2022	188	18	9,6%	1,7%

we used as well a dataset dedicated to spruce dieback due to bark beetle attacks.

5) Spruce Dieback Following Bark Beetle Crisis Using FORDEAD Method: Unprecedented levels of bark beetle infestations have been observed on spruce in France and other European countries since 2018. A method has been specifically developed to monitor spruce dieback caused by bark beetles, using Sentinel-2 time series analysis: anomalies are identified at a 10 m pixel size based on a reference defined by a harmonic model fitted on the seasonality of a spectral index over two reference years. This method is accessible via the FORDEAD python package. The spectral index used here is named CR_{SWIR}, a spectral index sensitive to vegetation water content. The CR_{SWIR} is obtained by applying a continuum removal to the near-infrared (NIR) and shortwave infrared (SWIR) domains of Sentinel-2 level 2A reflectance data (bands 8A, 11, and 12). Several studies identified water related spectral indices based on SWIR information as particularly relevant for early disturbance detection [31], [32], [33].

Here, we applied FORDEAD on the Sentinel-2 time series corresponding to the military grid reference system (MGRS) tile 31TEN (Bourgogne-Franche-Comté region). The BD Forêt V2 layer from the IGN reports 430 000 ha of forest in this tile, among which 22 556 ha correspond to spruce and conifers susceptible to bark beetle attacks. We used 2016 and 2017 as reference years to define pixelwise seasonality, as this period was prior to bark beetle attacks and massive tree dieback in this region. Then, we applied FORDEAD to monitor anomalies from 2020 to 2022. Most of the bark beetle attacks occurred in 2020, then strongly decreased.

We compared spruce dieback to clear-cuts detected in this study, analyzing the time difference between the first Sentinel-2 anomaly related to dieback or sanitary cut and the detection of clear-cuts from Sentinel-1.

C. Forest Masks Data

The dominant leaf type 2018 map from Copernicus Land Monitoring Service provides two classes: conifer and broadleaf forests, and is used to analyze clear-cuts areas over conifer and broadleaf forests. The TCD 2018 map is used for deriving a forest and nonforest mask. In addition, TCD was used together with the height map from [34] to statistically assess tree cover and height over clear-cuts areas. Note that TCD is a measure of the amount of ground covered by the vertical projection of tree crowns onto the ground surface, expressed in percentage.

D. Methods

1) Clear-Cuts Detection: The method used in this study to detect patches of clear-cuts is summarized in the flowchart in Fig. 2 and detailed below. The core of the method is the production of weekly clear-cuts detections.

The clear-cuts detection method is based to a large extent on the one described in [23]. It has been used since 2022 through the so-called TropiSCO operational system developed by the CESBIO, CNES, and GlobEO to detect forest loss at the large scale, accurately and in a timely manner. Forest loss maps are being produced every day whatever the meteorological conditions, at a 10 m pixel size and 0.1 ha minimum mapping unit, from 2018. The method, initially designed to map tropical forest loss, has been here adapted to detect temperate forests clear-cuts as follows.

First, we developed a forest and nonforest mask based on the TCD 2018 map from Copernicus Land Monitoring Service. To do so, we assumed as a forest definition a minimum tree cover of 10%, as adopted by the Food and Agriculture Organization.

The clear-cuts detection method is based on the application of the radar change ratio (RCR) [35], which consists of a ratio between the post- and predisturbance averaged backscatter. In practice, the changes that occur between date d_i and date d_{i+1} are measured by the ratio RCR $= M_a/M_b$ where M_b is the temporal mean backscatter in X_b images before and including date d_i, and M_a is the temporal mean backscatter in X_a images from and including date d_{i+1}. As detailed in [23], X_a was fixed at 3, which allows to reduce speckle effect and consequently false alarms but delays detections, compared to values of 1 and 2. When a new Sentinel-1 image is available, the detection delay ranges from 12 to 24 days with a six (configuration with two Sentinel-1 satellites) or 12 (one Sentinel-1 satellite) days. Then, the date corresponding to the lowest RCR value is considered as our estimate of the detected clear-cuts date if the lowest RCR value is smaller than a given threshold. Thresholding is composed of two main steps, both based on the use of the RCR indicator, 1) the detection of shadows that appear at the boundary between forest and clear-cuts areas in a series of images, and 2) the detection of the deforested patches associated with the shadows. This strategy can be described as an object-oriented segmentation procedure, which uses very low RCR pixels as

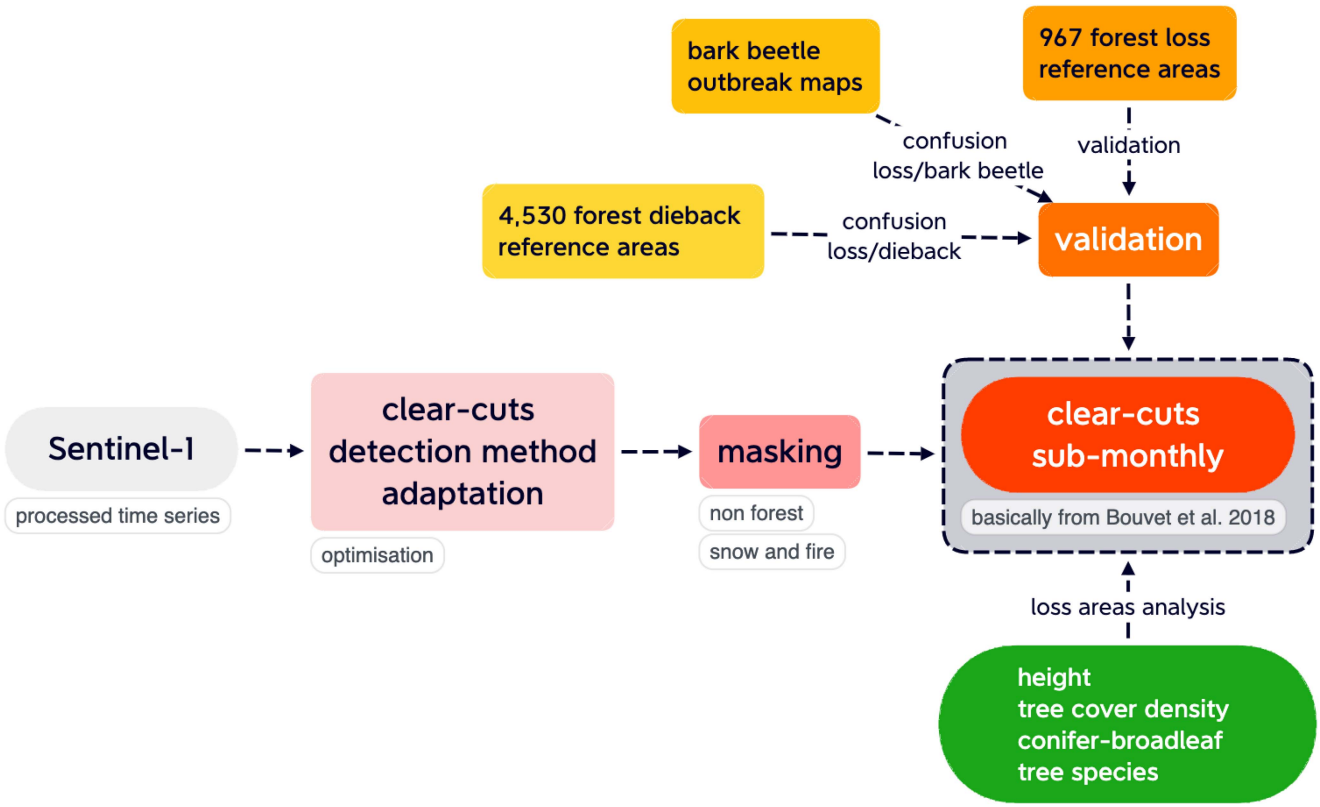

Fig. 2. Flowchart summarizing the main steps of the study.

seeds and extends segmentation through moderately negative values of RCR. The optimal RCR thresholds in [23], initially adapted to the tropics, were found to be $t_s = -4.5$ dB (t_s stands for shadows threshold) and $t_p = -3$ dB (t_p stands for patches threshold). Using the clear-cuts reference data described in Section II-B, we investigated in this study the need to adapt the two thresholds for temperate forests. Basically, adaptation may be due to differences in tropical and temperate forest structure and species, various environmental and meteorological conditions, etc. To do so, we applied to t_s and t_p a multiplicative threshold correction factor ranging from 0.8 to 1.2 with a 0.05 step. For example, a threshold correction factor of 1.1 would lead to $t_s = -4.95$ dB for shadows and $t_p = -3.3$ dB, i.e., to a stricter system with potentially fewer detections.

The adapted clear-cuts detection method was first applied to Sentinel-1 data acquired in 2019 over France mainland territory and Corsica. We used these 2019 detection results to update the forest and nonforest mask. This step is crucial to ensure better clear-cuts detection accuracy by improving the forest and nonforest mask quality. In fact, the system potentially detects targets with high backscatter variability, such as bare soil or crops that would be wrongly classified as forest into the forest and nonforest mask. After the forest and nonforest mask correction, we then applied the clear-cuts detection method on Sentinel-1 data acquired from January 2020 to July 2023. We then mosaicked and cleaned the resulting map using the following postprocessing steps. First, detections lower than 0.1 ha have been discarded to reduce the number of false alarms. Then, a closing morphological operation has been applied to slightly smooth detection areas. Then, we masked out detections under snow conditions from January 2020 to July 2023 using the monthly MODIS snow cover data based on a snow mapping algorithm that employs a normalized difference snow index, as snow was found to create false alarms due to associated strong backscatter decrease. For a given month, we calculate the surface area detected by the MODIS snow product (which is daily) and then we mask out the Sentinel-1 images for that month, which allow us to temporarily stop our detections. Any clear-cuts will then be detected with a maximum delay of one month. Finally, we used the EFFIS annual, high-resolution fire maps to mask out the detected objects that were affected by fire on 75% or more of its surface. We masked out fire areas because SAR backscatter can significantly decrease even when the forest remains alive, for example because of the undergrowth that burned. As for snow, fire masking is temporary and burnt forest that died or having been cut is then detected.

From the clear-cuts detection maps and ancillary data, we assessed annual and submonthly clear-cuts for broadleaf and conifer forests, for various tree species, and over public and private forests. In addition, we investigated the height and TCD distribution of forest before it was cut, and analyzed the temporal evolution of the size of clear-cuts areas.

2) Validation: As described above, the clear-cuts detection method employed here uses an object-based approach, analyzing and flagging clusters of data that share similar temporal behavior. Therefore, we adopted an object-based approach to

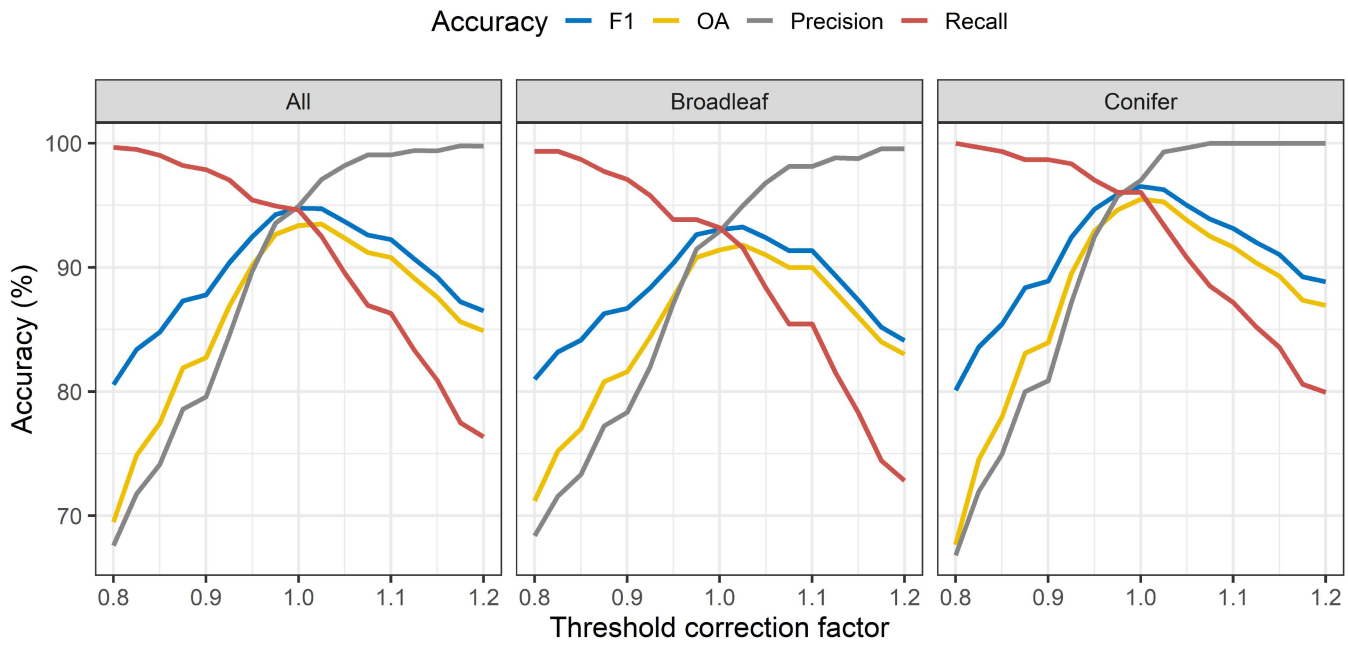

Fig. 3. Validation results depending on the threshold correction factor, over all types of forests, broadleaf, and conifer forests. OA, F1 score, precision, and recall are used as accuracy assessment indicators.

the validation procedures, following standard methods used on most machine-learning object-based algorithms. Specifically, we studied how the clear-cuts detection algorithm behaved over each one of the manually drawn reference polygons (see Section II-B). Given a set of detection parameters, we classified as being true positive (TP) or false negative (FN) each reference plot of the class "clear-cuts" that had more than 75% of its surface flagged as "deforested" by our algorithm. Similarly, we classified as a true negative (TN) or false positive (FP) each reference plot of the class "no clear-cuts" that had more than 75% of its surface nondetected by our algorithm. Once, all the TN, TP, FP, and FN values were computed for every set of detection parameters (see thresholds in Section II-D1), we computed a number of accuracy metrics as follows.

1) Recall that measures the ability of our system to correctly identify all the actual TP's instances, i.e., finding all clear-cuts areas in the map, out of the sum of TP and FN. High recall indicates that the system is good at not missing actual positive instances, whereas low recall means the system is missing some of them.
2) Precision, which is a measure of how well our system can correctly identify TP's without including too many FPs, and is defined as the ratio of TP by the sum of TP and FP. High precision means that the system is making positive predictions with a low rate of false alarms (FP).
3) Overall accuracy (OA), which calculates the proportion of all correctly classified cases (TP+TN) among all instances (sum of TP, TN, FP, and FN).
4) F1 score, which gives an overall measure that balances Precision and Recall and is defined as the harmonic mean of these two accuracy measures. A high F1 score allows to avoid either too many FPs or too many FNs.

The criteria we used for selecting the threshold correction factor was a recall higher than 80% with the highest possible precision value. In simple terms, we preferred fewer FPs at the cost of fewer TPs, to maximize the probability that a detected TP is actually true (fewer false detections at the cost of missing some clear-cuts).

For the sake of comparison, we applied this validation procedure to our maps and to annual forest loss maps from [4] and [29].

III. Results

A. Validation of Clear-Cuts Detection

A threshold correction factor ranging from 0.8 to 1.2 with a 0.05 step was applied to t_s and t_p as detailed in Section II-D. OA, F1 score, precision, and recall were then calculated for clear-cuts and intact forest (no clear-cuts) classes for each threshold correction factor. Validation results are shown in Fig. 3. The best OA and F1 scores were obtained for a threshold correction factor of 1. F1 is 94.7%, 93.1%, and 96.5% for all forests, broadleaf, and conifer forests, respectively. Conifer clear-cuts are better detected than broadleaf forests clear-cuts, which is explained by the fact that logged conifer are mostly homogeneous plantations with little seasonal effects on the backscatter. On the contrary, the inherent seasonality of deciduous broadleaf forests leads to variations of backscatter in time, which makes detection somewhat harder. The fact that best results were obtained for threshold correction factor of 1 means that the thresholds commonly used in tropical countries are well adapted to temperate forests, as shown in Fig. 3. The values of precision and recall then increase and decrease, respectively, with increasing threshold correction factor, meaning less FP and TP. The criteria we defined in Section II-D, i.e., recall higher than 80% with the highest possible

precision value, was fulfilled for a threshold correction factor of 1.15, which we thus used for deriving the final clear-cuts maps. The corresponding OA, F1, precision, and recall values over all forests are 87.6%, 89.2%, 99.4%, and 80.9%, respectively.

We conducted a quantitative comparison of clear-cuts surface areas derived from our approach with the findings from GFW [4], INRAE [17], and TUM [29]. It is important to note that we do not regard the maps produced by GFW, INRAE, and TUM as benchmarks, and our preference for using Sentinel-1 lies in its superior capability for timely forest detection. The corresponding OA, F1, precision, and recall values of GFW over all forests are 79.8%, 81.1%, 99.2%, and 68.5%, respectively. GFW shows a relatively constant estimate of forest loss, ranging between 700 and 800 km^2 depending on the year, which is more conservative than our system ($<$ 2000 km^2 each year). During the 2020–2022 period, GFW 2020–2022 forest loss data summed up to 282 765 ha, against 595 877 ha detected by our system. Regarding map agreement, GFW detected 37% of our system's detections, whereas our system covered 78% of GWF's detections. These numbers suggest a higher accuracy of our system, which seems to have a much lower omission than GFW. We also validated the latest results of [29] and compared their results with ours for the years 2020 to 2022. The OA, F1, precision, and recall values of [29] over all forests are 71.8%, 71.6%, 98.7%, and 56.1%, respectively, showing less accurate results than those from GFW. During the 2020–2022 period, forest loss maps from [29] summed up to 505 691 ha, which is close to the 595 877 ha detected by our system. The agreement numbers are 35% (Senf and Seidl detections of our data) and 41% (our system's detections over Senf and Seidl forest loss areas). We obtained INRAE's map over four MGRS tiles (30TXQ, 30TXP, 30TYQ, and 30TYP) in the Landes forest only, which represents approximately 30 000 km^2. From 2020 to July 2023, the INRAE system detected more clear-cuts areas compared to our system (579 889 versus 132 248 objects) but detected less clear-cuts surface area (77 660 versus 94 080 ha). This is due to the fact that INRAE's maps minimum mapping unit is smaller (0.01 versus 0.1 ha). The INRAE system detected 48% of our detections, whereas we detected 58% of INRAE's detections. These results show that the two maps might be complementary and could be jointly used. Note that we were not able to validate INRAE's map because the latter was not accessible outside of the Landes forests.

B. Annual and Submonthly Clear-Cuts Assessment

The validated methodology was applied to the entire mainland France, which represents approximately 543 940 km^2. All the processing was made using open-source packages and libraries, such as Xarray and Dask. Fig. 4 shows some examples of the results of the clear-cuts detection procedure.

The heatmaps corresponding to clear-cuts density from January 2020 to July 2023 for all forests, conifer and broadleaf, are shown in Fig. 5, and the corresponding estimated clear-cuts areas per region are summarized in Fig. 6. Clear-cuts surface area is estimated to be 1 995 km^2 in 2020, 1 970 km^2 in 2021, 1 984 km^2 in 2022, and 749 km^2 in the first half of 2023, which shows

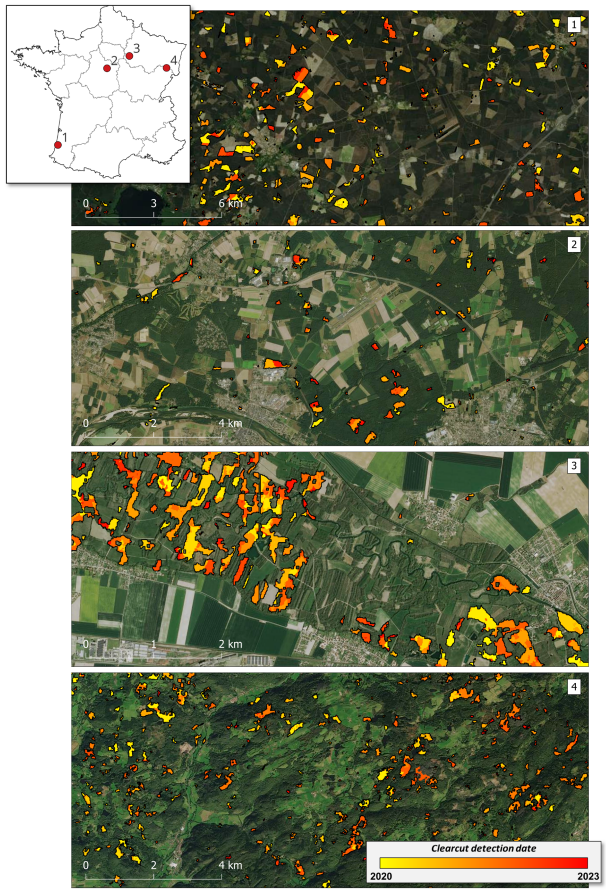

Fig. 4. Examples of clear-cuts mapped during this study. 1) Conifer forests cuts in the Landes region. 2) Public forest clear-cut near the city of Châteauneuf-sur-Loire, Orleans region. 3) Clear-cut related to poplar cultivation on the Seine river terraces, near the city of Troyes. 4) Montane forests clear-cut in the region of the Vosges. Background: 2021 SPOT Imagery delivered by the French national mapping agency (IGN).

remarkable stability over time. Clear-cuts in broadleaf forests is stable in 2020 and 2021 but increases in 2022 (1 163 km^2, 1 120 km^2, and 1 332 km^2, respectively). Figs. 5 and 6 highlight high variability of clear-cuts surface area among regions, forest type and time. The number of clear-cuts areas varies greatly from region to region, depending on the forest surface area per region and on whether the silviculture includes clear-cutting as a regeneration method or is dominated by natural regeneration. The three regions with the highest clear-cuts surface are the Nouvelle-Aquitaine region in South-West where the Landes forest is situated (2 070 km^2 in total from 2020 to July 2023, including 1 020 km^2 of conifer, and 1 050 km^2 of broadleaf), followed by Bourgogne-Franche-Comté located in Centre-East (920 km^2) and Auvergne-Rhône-Alpes (780 km^2). Corse is the region with the lowest amount of clear-cuts (16 km^2). After the Nouvelle-Aquitaine region, the highest number of conifer and broadleaf clear-cuts are located in Bourgogne-Franche-Comté (440 km^2) and Grand Est (490 km^2), respectively. Note that the bark beetle crisis in Grand-Est has led to the death of around 1 000 km^2 of conifer stands (mainly spruce and fir) since the crisis began in 2018. Most of these stands have been harvested (sanitary cuts) and probably detected by our system.

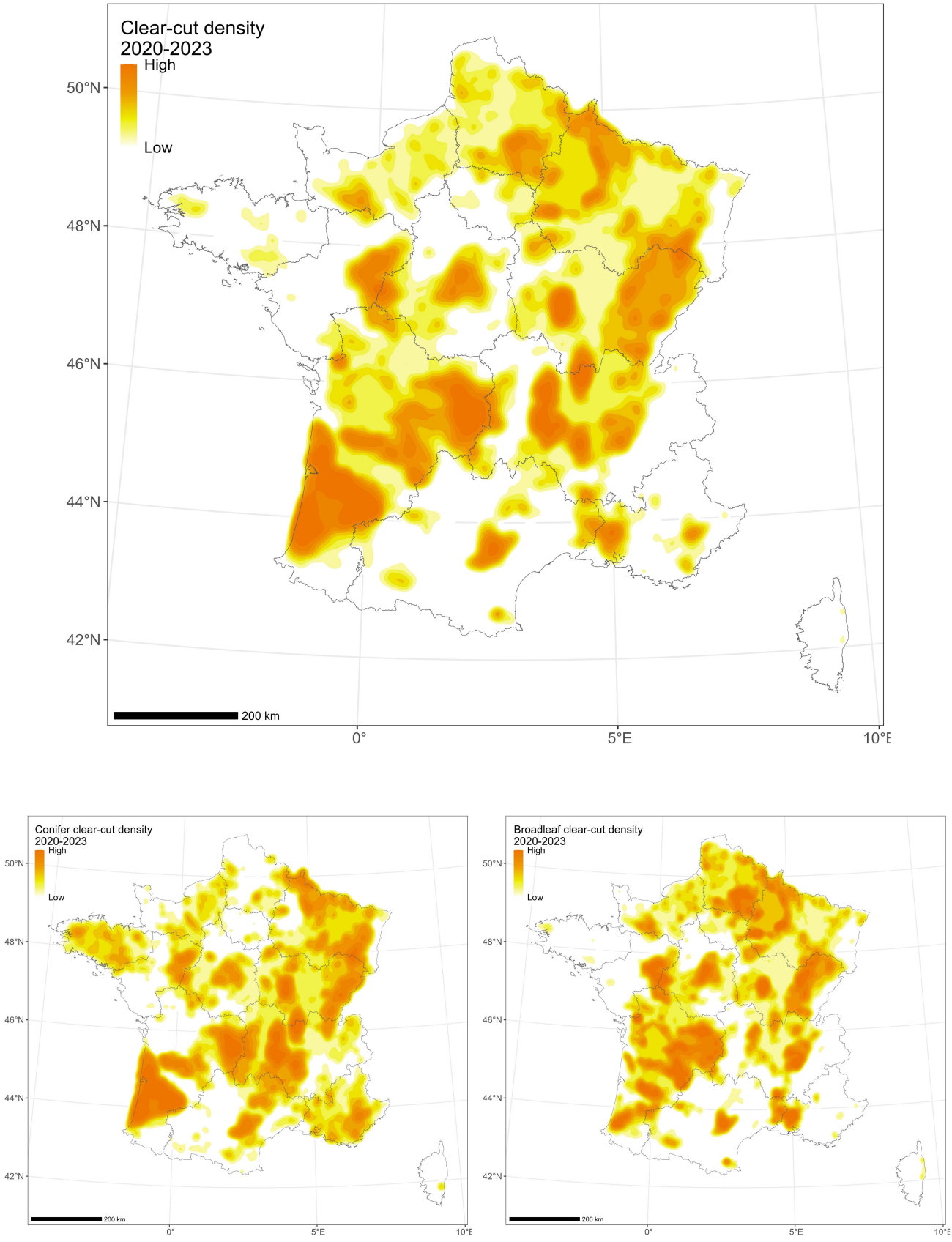

Fig. 5. Heatmaps from 2020 to July 2023 of clear-cuts for all forests (top), conifer (bottom left), and broadleaf (bottom right). In the color scale, *high* means 100% of probability of finding a 1 ha clear cut on a 6 km^2, *low* meaning 0% of probability of this event.

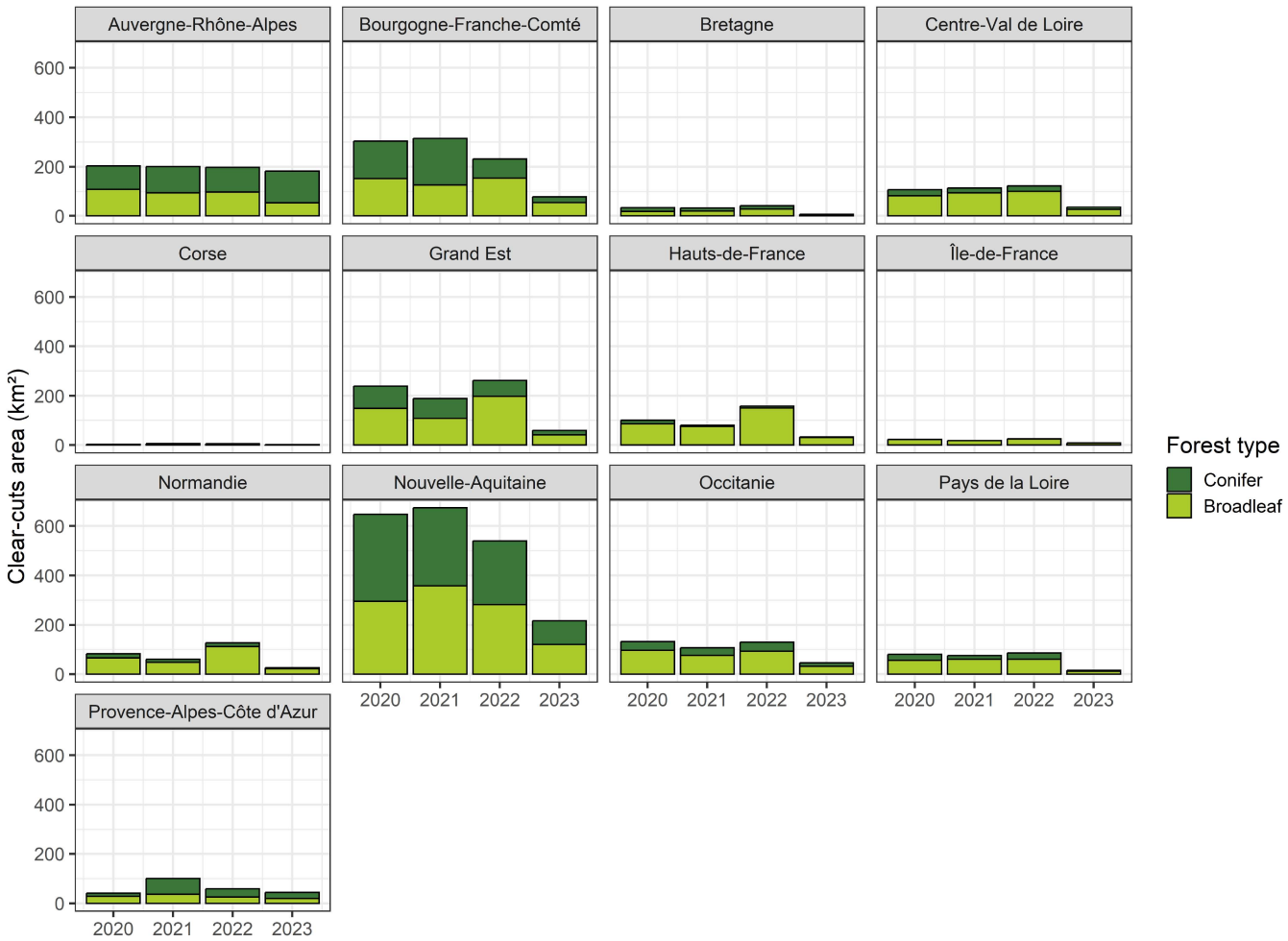

Fig. 6. Clear-cuts area for all forests, conifer and broadleaf forests per region and per year from 2020 to July 2023.

Clear-cuts in regions such as Corse, Hauts-de-France, and Île-de-France applies almost exclusively to broadleaf forests. Regions such as Auvergne-Rhône-Alpes exhibit stable clear-cuts area among years, whereas Provence-Alpes-Côte d'Azur exhibits much more conifer clear-cuts in 2021 (64 km^2) than in other years (12 km^2 in 2020).

The information on clear-cuts provided above is enriched with a new piece of information, the total forest area, in the bivariate map, shown in Fig. 7, for each French department and region. The total forest surface area is represented by colors from gray (small total forest surface area) to green (large total forest surface area). The clear-cuts surface area is represented by colors from gray (small amount of clear-cuts) to pink (large amount of clear-cuts). It is easy to see that Bretagne, shown in gray in Fig. 7, has a low proportion of forest surface area and clear-cuts. Corse has a lot of forest but little clear-cuts. However, large parts of Nouvelle-Aquitaine and Bourgogne-Franche-Comté, shown in dark red on the map, exhibit large forest areas with a lot of clear-cuts.

The annual clear-cuts estimations presented above were assessed from submonthly detections based on all Sentinel-1A images from 2020 to the first half of 2023. It is, therefore, possible to observe the subannual temporal evolution of clear-cuts. Fig. 8 shows the clear-cuts submonthly temporal evolution for all forests, conifer, and broadleaf for the whole of France (top) and per region (bottom), and Fig. 9 shows the clear-cuts temporal evolution per tree species. Regarding the whole of France, two clear-cuts peaks are observed every year approximately in February and March and June and July. In fact, the wood is usually harvested in late winter or in spring, but heavy machinery damages the soil when too soaked, in which case we harvest in summer. The period with the smallest amount of clear-cuts is between October and January, due to lower temperatures, more precipitations and in some cases the presence of snow. Trends between conifer and broadleaf forests are in general similar. The temporal evolution per region shows large variations in time. While Centre-Val de Loire, Île-de-France, and Pays de la Loire exhibit the same behavior as what is observed over the whole of France (two peaks per year and a similar amount of clear-cuts among years), Auvergne-Rhône-Alpes exhibit one peak at the beginning of 2020 and a very large one at the beginning of 2023. The latter is probably due to the sharp increase in bark beetle damage in this region in 2022 and 2023.

C. Clear-Cuts in Private and Public Forests

Approximately three-quarters of forests in France are private forests. Our quantification of clear-cuts reveals an estimated

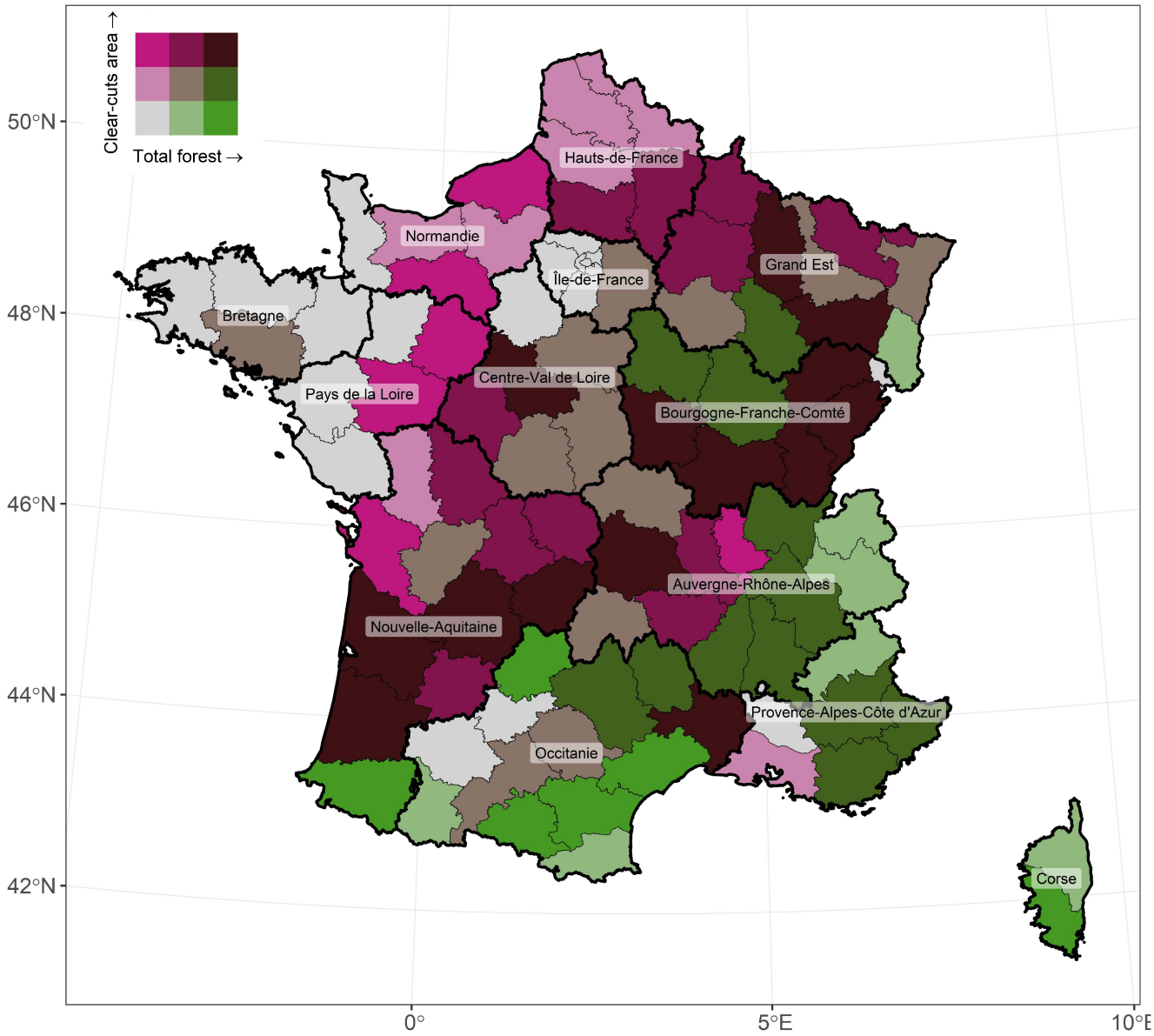

Fig. 7. Bivariate map showing clear-cuts areas from 2020 to July 2023 relative to total forest surface, per department, and region. The total forest surface area is represented by colors from gray (small total forest surface area) to green (large total forest surface area). Clear-cuts surface area is represented by colors from gray (small amount of clear-cuts) to pink (large amount of clear-cuts). Departments are separated by light black lines and regions by thick black lines.

extent of 5 850.1 km^2 within privately owned forested areas, in contrast to 848.2 km^2 observed in publicly owned forested regions. This discrepancy delineates a ratio of seven between the two categories, primarily due to extensive clear-cutting of maritime pine, a species found mainly in private forests (Nouvelle-Aquitaine). The variability of clear-cuts in private and public forests among regions can be observed in Fig. 10. The relative amount of clear-cuts in public forests versus private forests is negligible in many regions, such as in Auvergne-Rhône-Alpes, Bretagne, Centre-Val de Loire, Corse, Nouvelle-Aquitaine, and Pays de la Loire, for example. On the contrary, the share of public forests in the overall clear-cuts is almost one-third in Grand Est, and one-fourth in Bourgogne-Franche-Comté, and in Provence-Alpes-Côte d'Azur. In general, the proportion of conifer and broadleaf clear-cuts in private and public forests is similar. Bourgogne-Franche-Comté region represents a notable exception, as approximately half of the clear-cuts in private forests is broadleaf versus a third in public forests. In Provence-Alpes-Côte d'Azur, half of the clear-cuts in private forests is broadleaf versus two-thirds in public forests.

Our findings indicate that there are less clear-cuts in French public forests than private ones also when considered in relative terms (ratio of clear-cuts versus total forest by category). While private forests lost 2.15% of their surface from 2020 to July 2023, public forests only lost 0.89%. The regional results also show a double to triple fold difference between private and public clear-cuts (see Fig. 11). One notable exception is the Hauts-de-France region, where clear-cuts are almost equal and notable

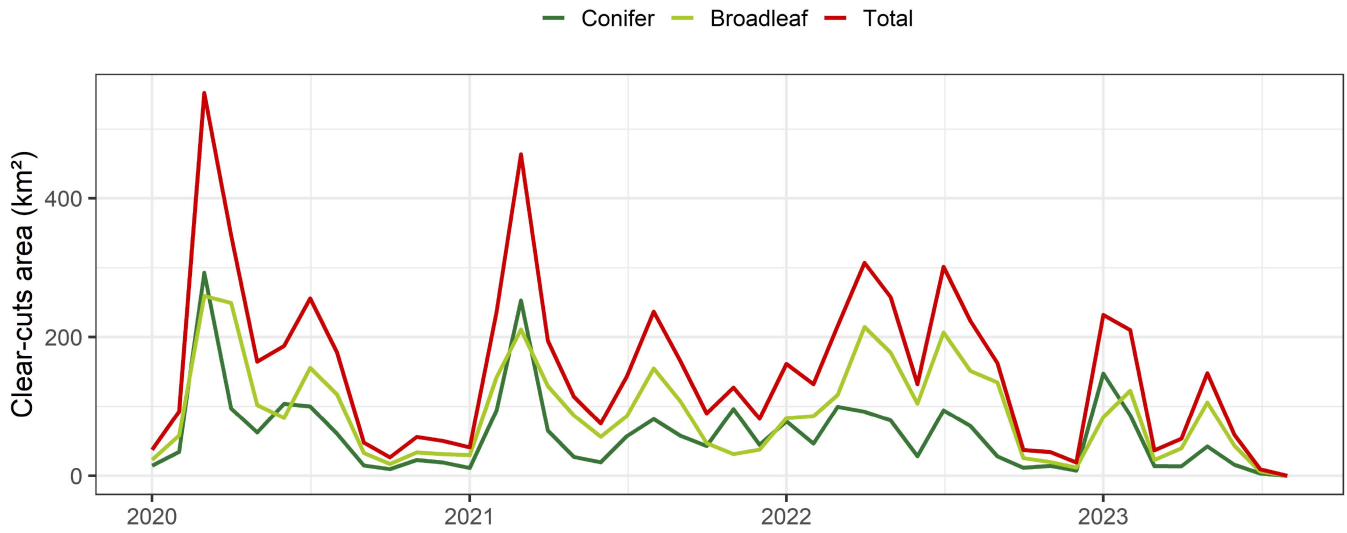

(a)

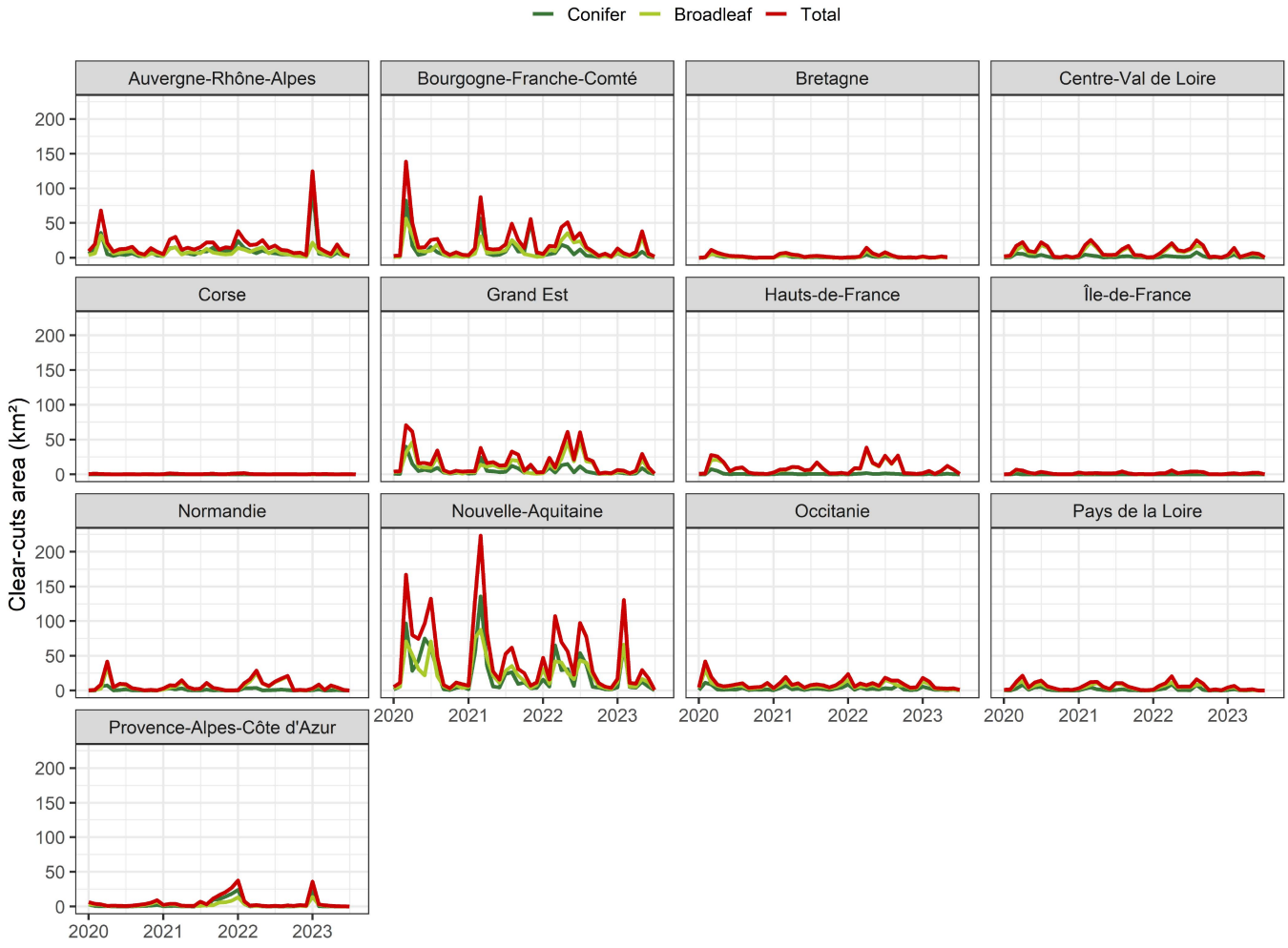

(b)

Fig. 8. Clear-cuts submonthly temporal evolution for all forests, conifer and broadleaf forests, (a) for the whole of France and (b) per region.

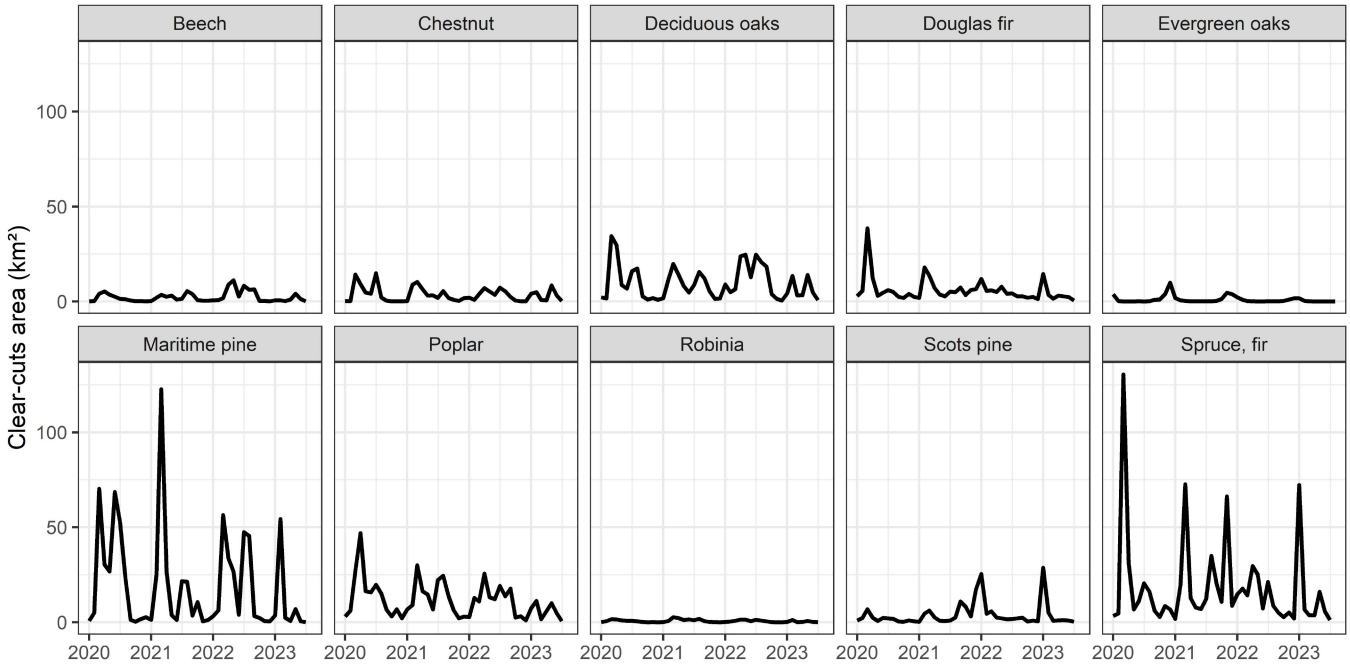

Fig. 9. Clear-cuts submonthly temporal evolution per tree species.

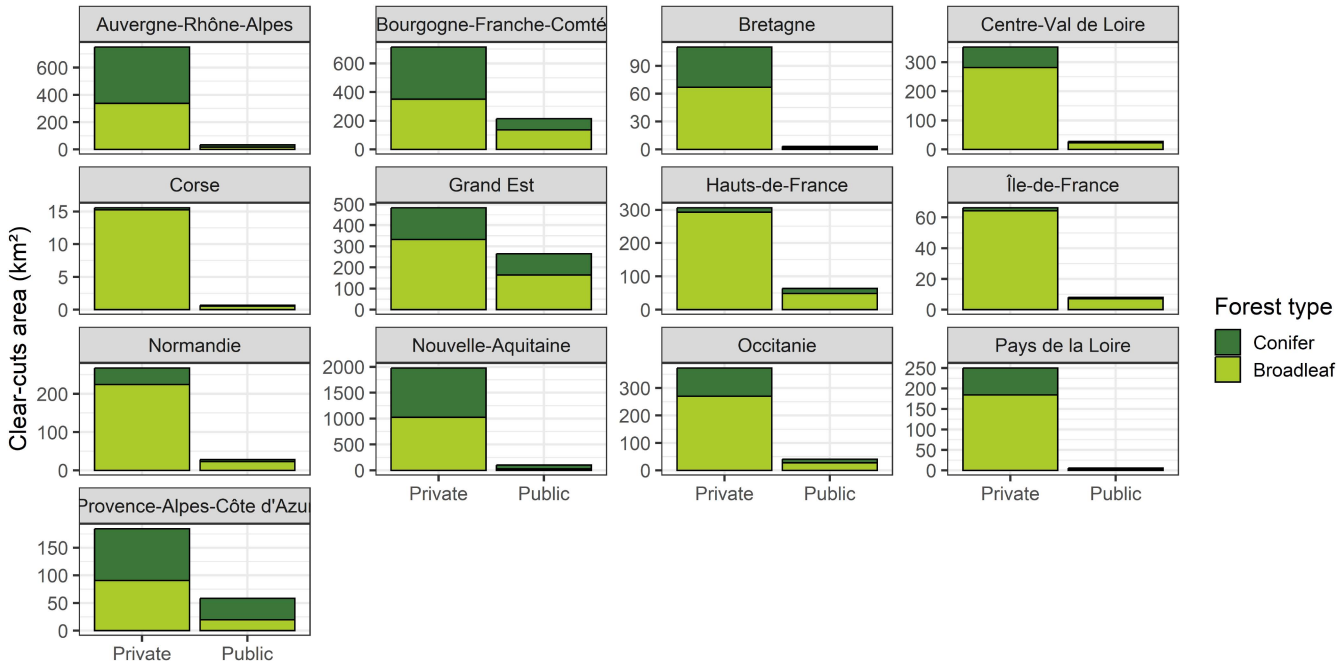

Fig. 10. Clear-cuts area per region for public and private forests.

high (around 5%). On the other side, the Corse region shows a very low relative index of clearings, especially over the public areas, where only 0.04% of the forest surface was cleared.

D. Clear-Cuts Per Tree Species

Clear-cuts have been separated by species for each year, using the BD Forêt V2 layer from the IGN, as shown in Fig. 12. IGN defines a pure stand when one tree species occupies more than 75% of the canopy in the dominant storey. As expected, maritime pine (*pin maritime*) is the identified tree species with the highest amount of clear-cuts (most of them being logged in the Landes forest), followed by spruce (*épicéa*), poplar (*peuplier*), and oak (*chêne*). Spruce logging is largely driven by the bark beetle crisis in France. In fact, France has faced significant clear-cuts due to bark beetle infestations exacerbated by exceptional dry weather conditions, especially in spruce populations, since few years. Oak logging also increased from 2020 (122.8 km^2) and 2021 (104.5 km^2) to 2022

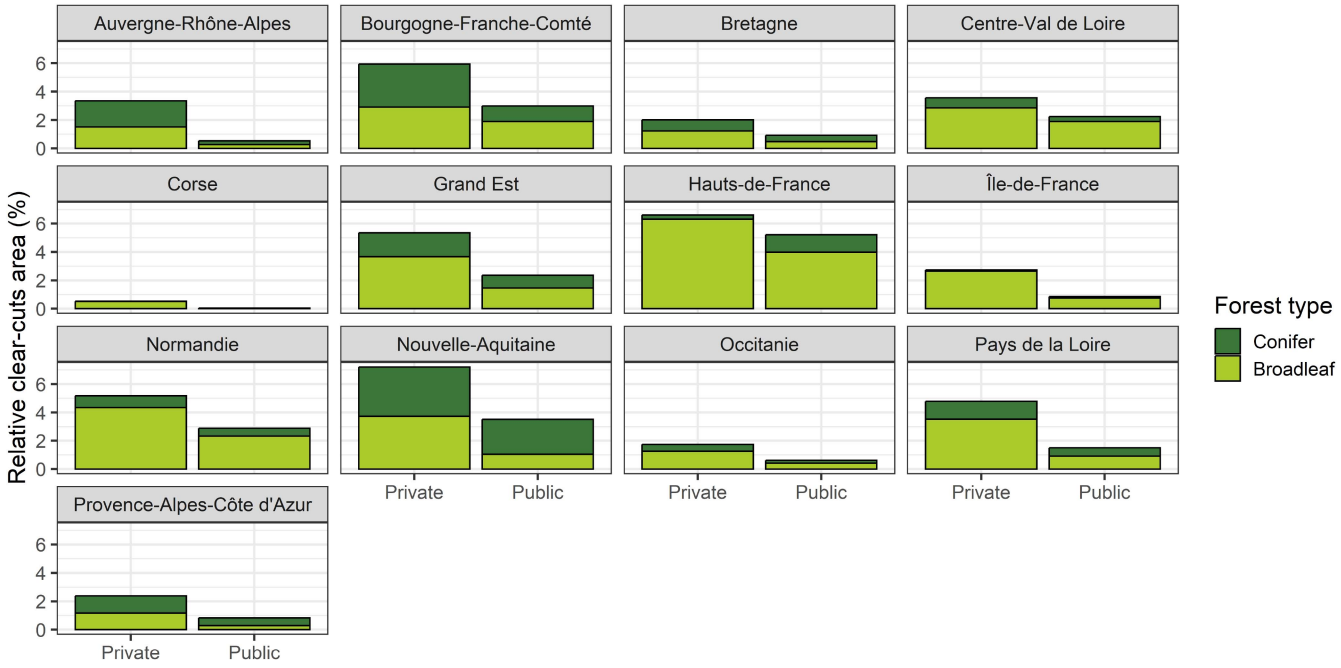

Fig. 11. Relative clear-cuts area per region for public and private forests (ratio of forest clear-cuts versus total forest by category).

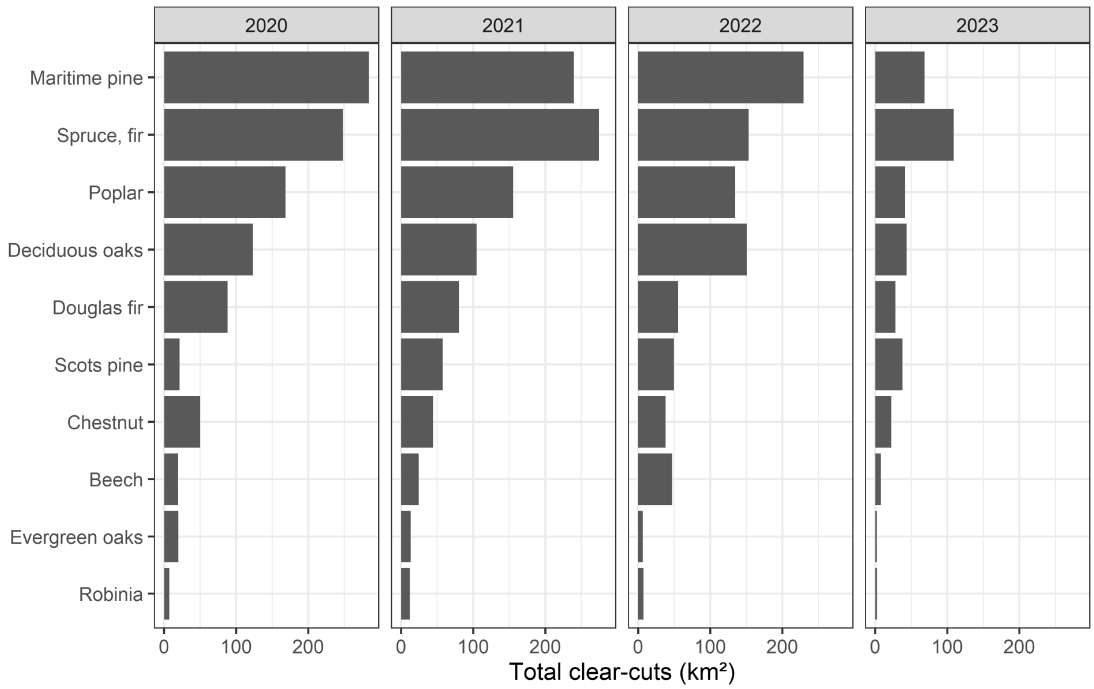

Fig. 12. Clear-cuts separated by species for each year, using the BD Forêt V2 layer from the French national mapping agency (IGN).

(150.7 km^2), probably linked to dieback, particularly in central France.

E. Height, TCD, and Size of Clear-Cuts Areas

In this section, statistics are related to forest height and TCD before clear-cuts are assessed. In addition, the size of clear-cuts areas is characterized.

Forest height of forest areas before disturbances per region and tree species are shown in Figs. 13 and 14. The mean and standard deviation of tree height in France is 19.6 m and 6.28 m. The mean tree height by region ranges between 11.4 and 20.5 m, being the two northeastern regions, Bourgogne-Franche-Comté and Grand Est, the ones where the mean tree height exceeds 20 m. As a reminder, these two regions have broadleaf and conifer forests in approximately similar proportions and

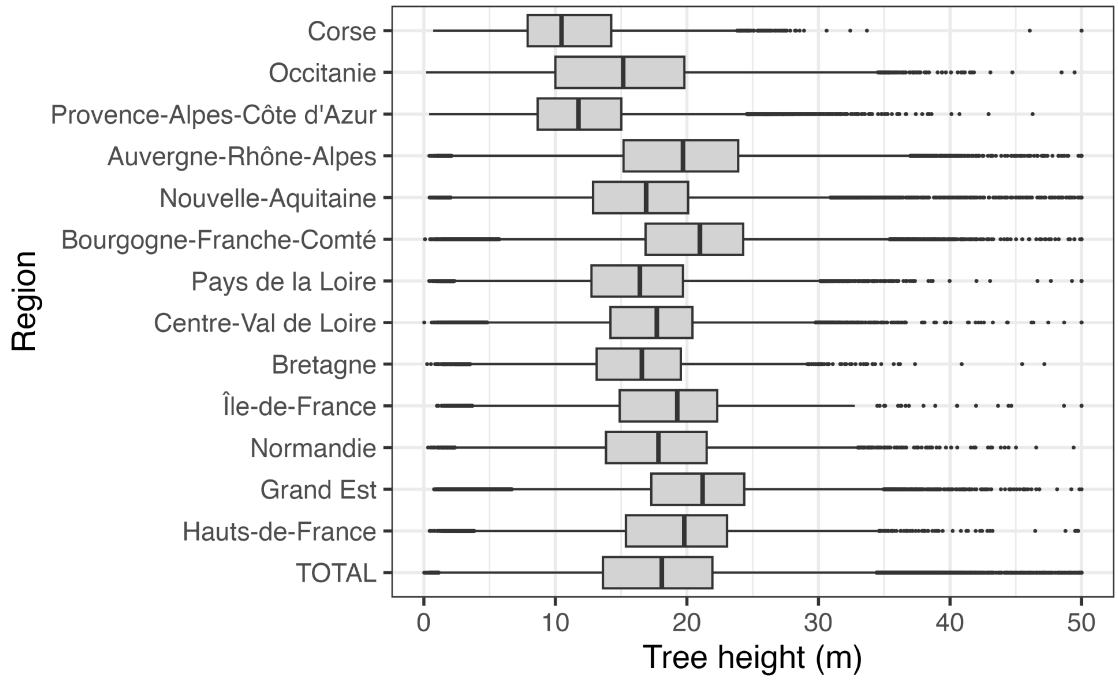

Fig. 13. Height statistics of clear-cuts areas in France from 2020 to July 2023 for all forests.

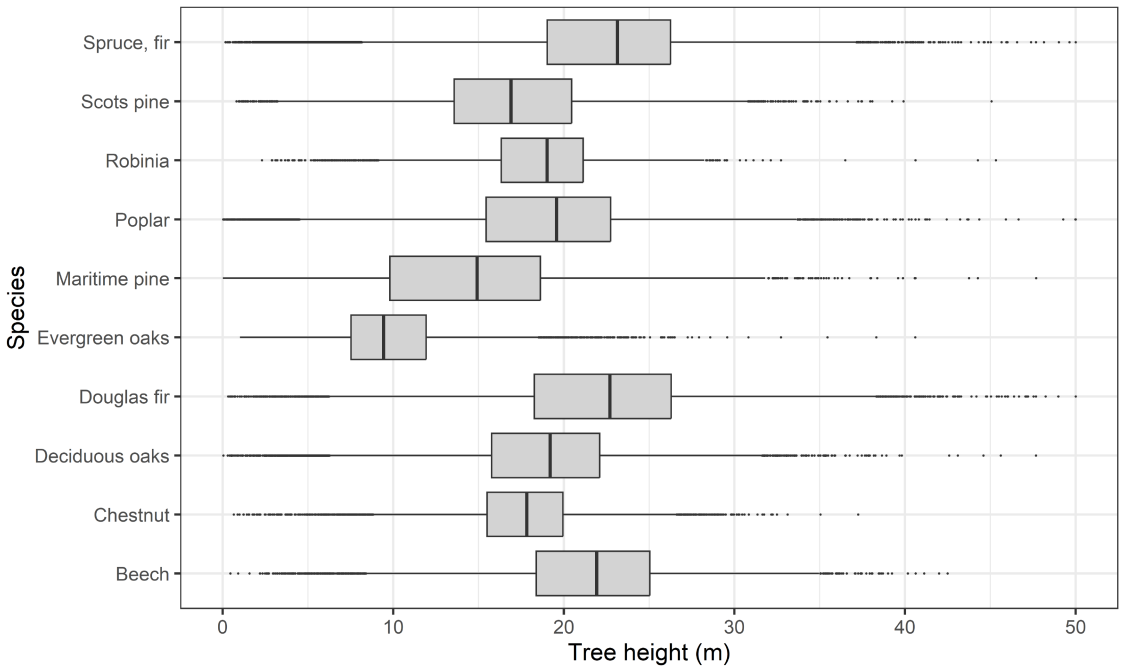

Fig. 14. Height statistics of clear-cuts areas in France from 2020 to July 2023 per tree species.

in Grand Est, the private forest is underrepresented (44%) compared to the national average (75%). TCD of forest areas before disturbances per region and tree species are shown in Figs. 15 and 16. The mean TCD of clear-cuts areas in France is 74%. The mean TCD per region ranges between 50% and 90%. The proportion of clear-cuts in 25% increments, i.e., from 0 to 25%, 25% to 50%, 50% to 75%, and 75% to 100%, is 4.9%, 12.6%, 31.3%, and 51.2%, respectively. These findings are not supported by national statistics and reflect the fact that the method is adapted to the detection of clear-cut involving the entire or a substantial part of the stand, as stated in Section I. The heights and TCD by species are generally consistent. However, the heights are somewhat low for maritime pine, poplar, and chestnut, which demonstrates a slight underestimation of the height map used. Another explanation could be that the clear cuts also involve simple coppices.

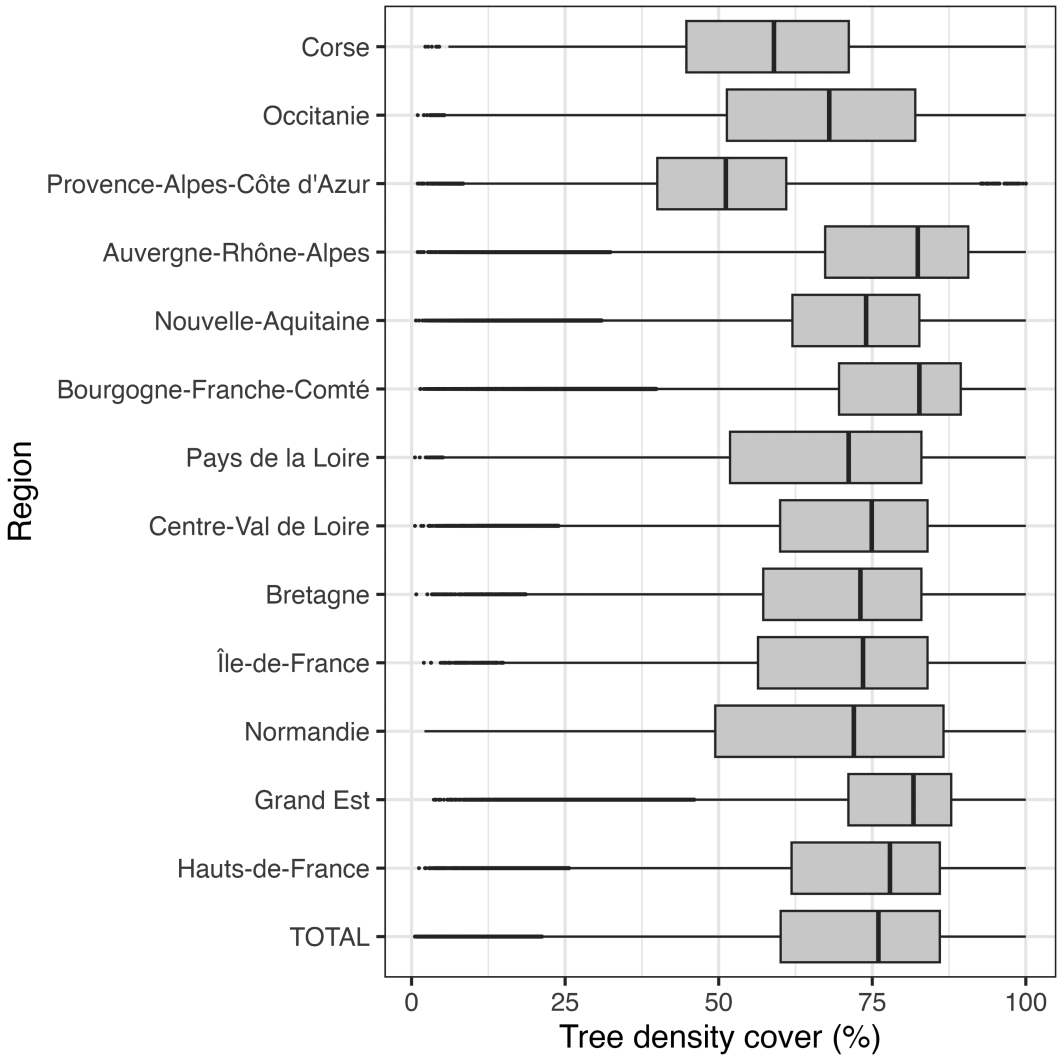

Fig. 15. TCD statistics of clear-cuts areas in France from 2020 to July 2023 for all forests.

The annual distribution of the size of clear-cuts areas is shown in Fig. 17. The size of clear-cuts areas is mostly smaller than 10 ha (for 98.7% of all clear-cuts areas). Half of clear-cuts are smaller than 0.45 ha. Interestingly, the mean size in 2020, 2021, 2022, and 2023 is 1.63, 1.29, 1.04, and 1 ha, respectively, i.e., decreasing in time. In some french departments, this reduction in the size of clear-cuts could be linked to thresholds set by the local government (Prefect) for cuts removing more than 50% of the volume of trees in the forest.

F. Influence of Forest Dieback on Clear-Cuts Detection

The areas of clear-cuts detected by our system were compared with 4 530 plots labeled in different campaigns. The results of our comparison are shown in Table II. Our approach is not impacted by forest dieback for the different species analyzed and confusions are very low.

It can be seen in Table II that most of the dieback plots are actually not detected as clear-cuts. Beech and chestnut (2022) forests have the largest confusion percentage with 5.4% and 9.6%, respectively, which represent only 0.8% and 1.7% of the percentage of dieback detected area versus total area. Only 10 oak dieback plots were detected as clear-cuts (0.3% of dieback plots, 0.1% when looking at the detected areas versus total area), which is interesting since oak is one of the most common trees in France. Among the 10 oak plots with areas detected as clear-cuts, only two of them have more than 50% of the plot surface area detected as clear-cuts. In conclusion, only 1.6% of dieback plots were detected as clear-cuts. These results show that our approach is not impacted by forest dieback for the different species analyzed. However, a clear-cut of a forest that died because of a dieback should be detected.

G. Comparison Between Clear-Cuts and Spruce Dieback Caused by Bark Beetle Attacks

The temporal evolution of clear-cuts monitored over spruce experiencing bark beetle attacks is reported in Table III. The peak dieback resulting from FORDEAD analysis occurred in 2020 (results from previous years not shown), then reduced by 60% to 70% in 2021 and 2022. Overall, 3 744 ha of spruce distributed over the Sentinel-2 tile (17% total spruce area) were identified

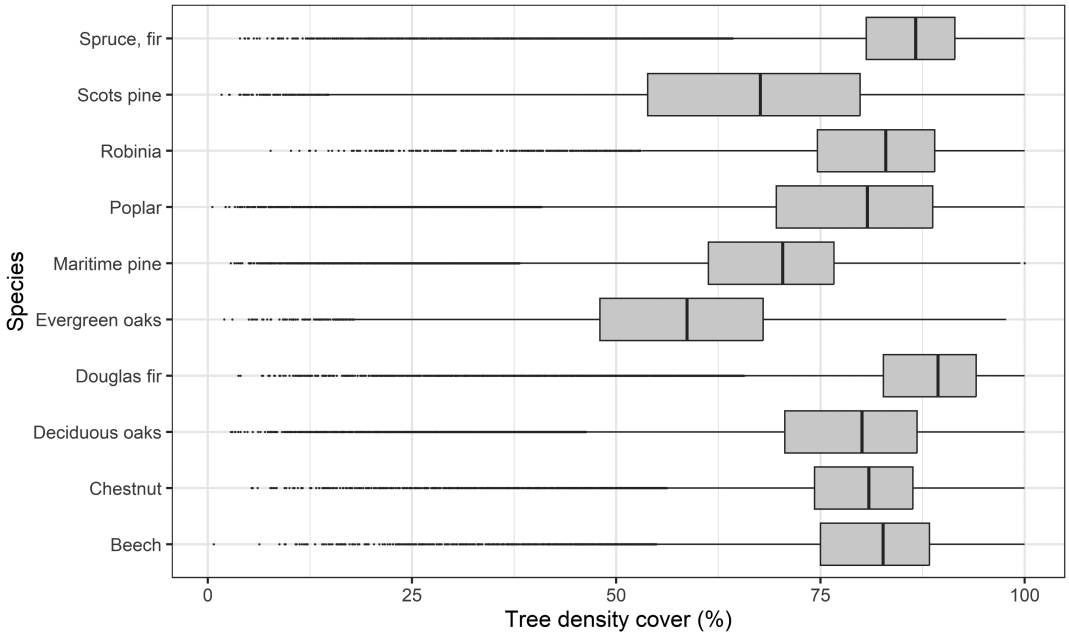

Fig. 16. TCD statistics of clear-cuts areas in France from 2020 to July 2023 per tree species.

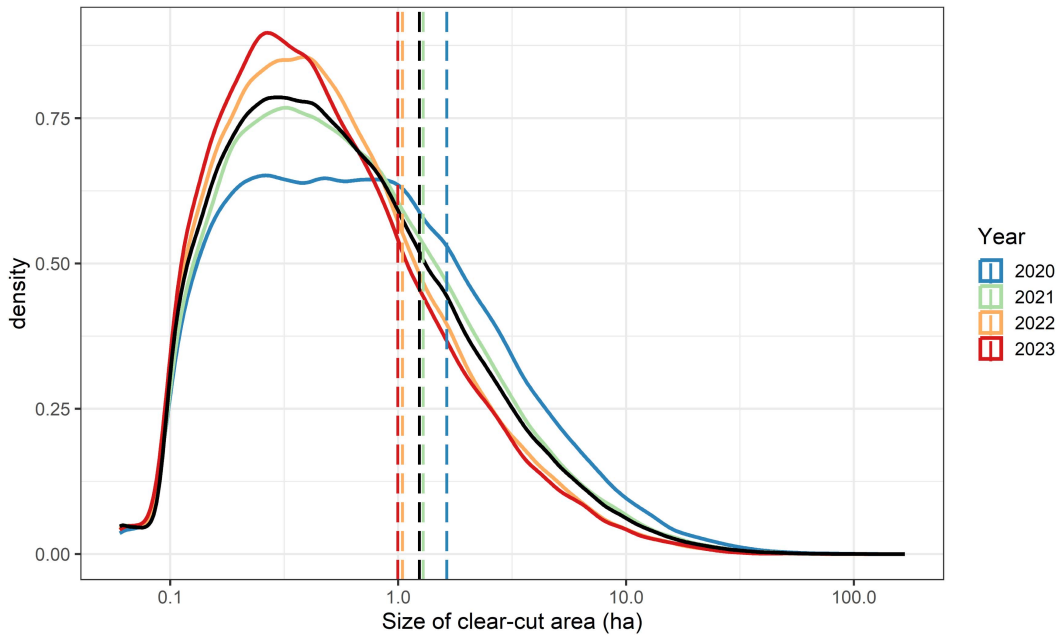

Fig. 17. Size statistics of clear-cuts areas in France from 2020 to July 2023 for all forests.

TABLE III
TEMPORAL EVOLUTION OF CLEAR-CUTS OCCURRING AFTER ANOMALIES RELATED TO BARK BEETLE ATTACKS ON SPRUCE FORESTS FROM 2020 TO 2022

	Clearcuts 2020–2023 (ha)	D_0	D_0 + 3 months	D_0 + 6 months	D_0 + 1 year	D_0 + 2 years
2020	1416	1.9%	17.2%	32.2%	61.7%	91.2%
2021	533	7.5%	35.4%	55.3%	84.9%	98.5%
2022	451	18.3%	40.6%	56.6%	93.9%	100.0%
2020-2022	2400	6.2%	25.6%	41.9%	72.9%	94.5%

Anomalies were detected with FORDEAD on Sentinel-2 tile T31TEN. D_0 corresponds to the day of the first anomaly identified with FORDEAD. Clearcuts is expressed as a % of total clearcuts for each year

as potentially impacted by bark beetle between 2020 and 2022. During the same period, 6.2% of detected bark beetle attacks were reported as clear-cuts at the same time (D_0), which can be considered as discrepancies.

Discrepancies between clear-cuts identified with Sentinel-1 and FORDEAD bark beetle attacks identified with Sentinel-2 may occur. In particular, pixels can be identified as clear-cuts prior to FORDEAD anomalies detection for the following reasons:

1) Clear-cuts may result from sanitary cuts impacting healthy stands neighboring diseased stands. FORDEAD anomalies will then be detected from clear sky Sentinel-2 acquisitions following clear-cuts. Such detections may be delayed for several weeks during cloudy conditions (e.g., winter), compared to forest loss identification with Sentinel-1.
2) Discrepancies may also occur for pixels at the border between healthy forested areas and stands with forest dieback or sanitary cuts.

Our results show that the occurrence of clear-cuts prior dieback detection remained very limited in 2020 (1.9%), and increased in 2021 (7.5%) and 2022 (18.3%), with 6.2% in total from 2020 to 2022. Most discrepancies for year 2021 correspond to clear-cuts less than one month before anomalies were detected with FORDEAD, which suggests sanitary cuts performed during winter at the peak of the bark beetle crisis. On the other hand, the relatively high proportion of clear-cuts occurring before anomaly detection with Sentinel-2 in 2022 (18.3%) may be caused by border effect between healthy and declining forests or sanitary cuts. More investigations are needed to conclude on these differences between Sentinel-1 and Sentinel-2.

Note that FORDEAD detects both diebacks and clear-cuts. However, we assume here the hypothesis that FORDEAD detections prior to those of this study are predominantly bark beetle attacks for two reasons. First, we tested FORDEAD in the Bourgogne-Franche-Comté region, which was heavily affected by bark beetle attacks between 2020 and 2022, as indicated in Section II-B5. Second, at time D_0, 6.2% of FORDEAD anomalies were detected by our system. If these were clear-cuts, our system would have detected much more than 6.2% since 80% of clear-cuts were accurately detected during the validation process. Moreover, many sanitary cuttings following bark beetle attacks occurred until 2022, which explains why the 6.2% increases to 94.5% after two years.

Overall, these results show that strong anomalies identified by FORDEAD, related to spruce dieback following bark beetle attacks, were relatively little identified as clear-cuts, which suggests that forest dieback could be distinguished from clear-cuts by Sentinel-1 to a certain extent. The proportion of forested surfaces identified as clear-cuts following dieback was 72.9% for the period from 2020 to 2022 at D_0 + 6 months, which was consistent with statistics reported by French authorities. In addition, clear-cuts identified by our system logically occurred after diebacks observation.

IV. Discussion

IGN provides every year a memento that is an overview of metropolitan France's forests status. This memento is based on the main results of the inventory data collected in the field over the previous five years. The last memento published in 2023 is based on almost 70 000 field plots inventoried from 2018 to 2022, including 14 000 plots observed in 2022. According to this memento, over the period 2013–2022, an average of 6 000 km^2 of production forest per year was cut: 600 km^2 concerned by a cut of more than 90% of the canopy, 250 km^2 affected by a cut of between 50% and 90% of the canopy, 1 900 km^2 affected by a cut between 15 and 50% of the canopy, and 3 200 km^2 affected by a cut of less than 15% of the canopy. As stated in Section III-B, we found in this study clear-cuts surface area of 1 995 km^2 in 2020, 1 970 km^2 in 2021, 1984 km^2 in 2022, and 749 km^2 in the first half of 2023. In one year, the amount of detected areas corresponds to the total area of cuts of more than 50% of the canopy (850 km^2), plus more than half of the 1 900 km^2 affected by a cut between 15% and 50%. We probably detect a very small portion of the 3 200 km^2 affected by a cut of less than 15% of the canopy.

Estimated clear-cuts surface area shows remarkable stability over time. However, clear-cuts in broadleaf forests is stable in 2020 and 2021 but increases in 2022 (1 163 km^2, 1 120 km^2, and 1332 km^2, respectively). Oak cutting in particular increased from 2020 (122.8 km^2) and 2021 (104.5 km^2) to 2022 (150.7 km^2). This trend can be partly explained in the light of oak dieback crisis and market prices. According to the France Bois Forêt Economic Observatory 2023 report, the average price of standing timber sales in 2022 rose by 17% to 94€/m^3 (highest level ever), compared with 81€ /m^3 in 2021, 61€ /m^3 the previous year, and systematically lower than 60€ /m^3 before 2017, except in 2007. This trend is mostly driven by oaks. In fact, after exceeding 200€ /m^3 for the first time in 2021, a new price record for oak in 2022, with an average price of 271€ /m^3 (for a unit volume of 1.7 m^3), an increase of 20% compared to 2021. This confirms the trend recorded since 2012. It is important to note that the period 2020–2022 is atypical.

We found seven times more clear-cuts in private forests than in public forests, although the surface area of private forests is only three times that of public forests. This can be explained by the fact that private forests are owned by many different individuals and companies with potential economic objectives such as selling timber. The demand for wood and forest products and the wood price increase can put economic pressure on private forest owners to cut. That is why short-rotation tree species (such as pine, poplar, etc.) in private forests are favored compared to public forests. On the other hand, public forests are generally managed by the state or other public entities such as the French National Forest Office (ONF), and their objectives may be more oriented toward long-term conservation and environmental protection with stricter regulations. In addition, some public forests are protected.

Interestingly, the cut area mean size in 2020, 2021, 2022, and 2023 is 1.63, 1.29, 1.04, and 1 ha respectively. This decreasing trend has been also observed from the most recent national inventory [36]. The fact that half of clear-cuts are smaller than 0.45 ha is an important result for environmental issues. Indeed, small cuts can sometimes be more favorable to ecological connectivity as they may leave buffer zones between deforested areas, facilitating the movement of species. Small cuts may

maintain a greater diversity of habitats, which can be beneficial for biodiversity. In addition, small cuts may allow for faster tree regeneration as some species can take advantage of favorable light and soil conditions. This shows that, in a context that is sometimes fraught with conflict between foresters and environmentalists, many foresters practice small, more environmentally friendly cuts.

Using optical data, the distinction between types of disturbance is fairly recent and still challenging [37], and requires the use of several complementary indices [38], [39]. The statistics derived generally include forest felling whatever the purpose, including damage caused by storms, fires, and any other phytosanitary problem. On the contrary, we showed that our radar-based system is not sensitive to phytosanitary dieback but only to clear-cuts following it. Standing dead trees, therefore, cannot be detected using SAR data, contrary to clear-cuts. In addition, fires are flagged and not retained in the clear-cuts maps from our system. Our maps are, therefore, complementary with the maps of dieback forests [30] and probably bark beetle damages [40].

ONF monitoring of forests under the forestry regime confirms a significant increase in felling in 2020 and 2021, linked to sanitary problems (bark beetles on spruce in particular). This phenomenon has also been observed in private forests. This may explain the high level of spruce clear-cuts we found in 2020 and 2021 (see Fig. 12). IGN also highlighted a constant increase of clear-cuts due to dieback [25].

In France, there are several systems in place to monitor clear-cutting operations. These systems are based on different methods and pursue different objectives (inventory, operational monitoring, and initial diagnosis for government departments). Some operational systems are based on observations made in the field (NFI, ONF monitoring of felling in public forests), whereas others rely on remote sensing and satellite image processing, such as [4]. It is possible to develop an optimal operational monitoring method that simultaneously draws on 1) field data (IGN in the first instance, but also ONF) because of their accuracy in terms of typology, and 2) remote sensing data providing high spatial coverage and frequent temporal information such as those from this study. In fact, field and satellite data respective strengths are complementary.

V. Conclusion

It is increasingly important to have access to accurate and up-to-date information on European forests. In this study, we adapted a Sentinel-1 based near real-time tropical forest loss detection method maps, which we applied to detect French temperate forests clear-cuts. The results exhibited recall and precision metrics of 80.9% and 99.4%, respectively. The fact that the highest OA was achieved with a threshold correction factor of 1 suggests that the thresholds typically used in tropical countries are also well suited for temperate forests. Using 4 530 reference data of dieback forests and maps of forest attacked by bark beetle, we also showed that forests with dieback were little confused with clear-cuts detections.

We found in this study a clear-cuts surface area of 1 995 km^2 in 2020, 1 970 km^2 in 2021, and 1 984 km^2 in 2022, which show remarkable stability over time. In one year, the detection system used here allows to detect areas affected by a cut of more than 50% of the canopy (850 km^2), plus more than half of the 1 900 km^2 affected by a cut between 15 and 50%.

We found seven times more clear-cuts in private forests than in public forests, although there are only three times more private than public forests, mainly for economic purposes.

The main perspective of this work is to develop a national statistical method that simultaneously draws on field data-based systems and our remote sensing-based system, as their strengths and weaknesses are highly complementary.

In addition, these analyses are probably reproducible to the rest of Europe, although the method needs to be tested for assessing transferability. These findings hold substantial significance for the progression of a radar-based system tailored for the near real-time detection of extensive disturbances in European temperate forests.

Acknowledgment

The Copernicus Land Monitoring Service maps are the property of the European Union, Copernicus Land Monitoring Service 2023, and the European Environment Agency (EEA). The authors would like to deeply thank ONF, DSF, INRAE, and Kenji Osé for sharing reference data. The authors would also like to thank the reviewers who did, in our opinion, a fantastic job and significantly improved this article.

References

[1] D. Wheeler, D. Hammer, R. Kraft, and A. Steelr, "Satellite-based forest clearing detection in the Brazilian Amazon: FORMA, DETER, and PRODES," 2014, Accessed: Oct. 15, 2023. [Online]. Available: https://www.wribrasil.org.br/sites/default/files/forma-issue-brief_1.pdf

[2] L. Reymondin et al., "A methodology for near real-time monitoring of habitat change at continental scales using MODIS-NDVI and TRMM," 2012, Accessed: Oct. 12, 2023. [Online]. Available: www.terra-i.org/dam/jcr:508a0e27-3c91-4022-93dd-81cf3fe31f42/Terra-i%20Method.pdf

[3] C. G. Diniz et al., "Deter-B: The new amazon near real-time deforestation detection system," *IEEE J. Sel. Topics Appl. Earth Observ. Remote Sens.*, vol. 8, no. 7, pp. 3619–3628, Jul. 2015.

[4] M. C. Hansen et al., "High-resolution global maps of 21st-century forest cover change," *Science*, vol. 342, no. 6160, pp. 850–853, 2013.

[5] M. C. Hansen et al., "Humid tropical forest disturbance alerts using landsat data," *Environ. Res. Lett.*, vol. 11, no. 3, 2016, Art. no. 034008.

[6] M. Ballère et al., "SAR data for tropical forest disturbance alerts in French Guiana: Benefit over optical imagery," *Remote Sens. Environ.*, vol. 252, 2021, Art. no. 112159.

[7] M. Watanabe, C. N. Koyama, M. Hayashi, I. Nagatani, and M. Shimada, "Early-stage deforestation detection in the tropics with L-band SAR," *IEEE J. Sel. Topics Appl. Earth Observ. Remote Sens.*, vol. 11, no. 6, pp. 2127–2133, Jun. 2018.

[8] M. Watanabe, C. N. Koyama, M. Hayashi, I. Nagatani, T. Tadono, and M. Shimada, "Refined algorithm for forest early warning system with alos-2/palsar-2 scansar data in tropical forest regions," *Remote Sens. Environ.*, vol. 265, 2021, Art. no. 112643.

[9] J. Reiche et al., "Forest disturbance alerts for the Congo basin using sentinel-1," *Environ. Res. Lett.*, vol. 16, no. 2, 2021, Art. no. 024005.

[10] S. Mermoz, A. Bouvet, T. Koleck, M. Ballére, and T. L. Toan, "Continuous detection of forest loss in Vietnam, Laos, and Cambodia using sentinel-1 data," *Remote Sens.*, vol. 13, no. 23, 2021, Art. no. 4877.

[11] J. Doblas et al., "Deter-R: An operational near-real time tropical forest disturbance warning system based on sentinel-1 time series analysis," *Remote Sens.*, vol. 14, no. 15, 2022, Art. no. 3658.

[12] J. Doblas et al., "Inter-comparison of optical and SAR-based forest disturbance warning systems in the Amazon shows the potential of combined sar-optical monitoring," *Int. J. Remote Sens.*, vol. 44, no. 1, pp. 59–77, 2023.

[13] C. Dupuis, A. Fayolle, J.-F. Bastin, N. Latte, and P. Lejeune, "Monitoring selective logging intensities in Central Africa with sentinel-1: A canopy disturbance experiment," *Remote Sens. Environ.*, vol. 298, 2023, Art. no. 113828.
[14] H. Carstairs et al., "Sentinel-1 shadows used to quantify canopy loss from selective logging in Gabon," *Remote Sens.*, vol. 14, no. 17, 2022, Art. no. 4233.
[15] B. Slagter et al., "Monitoring direct drivers of small-scale tropical forest disturbance in near real-time with sentinel-1 and-2 data," *Remote Sens. Environ.*, vol. 295, 2023, Art. no. 113655.
[16] S. Francini, R. E. McRoberts, and G. Chirici, "Near-real time forest change detection using planetscope imagery," *Eur. J. Remote Sens.*, vol. 53, no. 1, pp. 233–244, 2020, doi: 10.1080/22797254.2020.1806734.
[17] K. Osé and R. Cresson, "Clear-cuts detection services for the monitoring needs of the french ministry of agriculture," in *Proc. IEEE Int. Geosci. Remote Sens. Symp.*, 2019, pp. 4284–4287.
[18] J. C. White et al., "Confirmation of post-harvest spectral recovery from landsat time series using measures of forest cover and height derived from airborne laser scanning data," *Remote Sens. Environ.*, vol. 216, pp. 262–275, 2018.
[19] T. Hermosilla, M. A. Wulder, J. C. White, N. C. Coops, and G. W. Hobart, "Regional detection, characterization, and attribution of annual forest change from 1984 to 2012 using landsat-derived time-series metrics," *Remote Sens. Environ.*, vol. 170, pp. 121–132, 2015.
[20] J. C. White, M. A. Wulder, T. Hermosilla, N. C. Coops, and G. W. Hobart, "A nationwide annual characterization of 25 years of forest disturbance and recovery for Canada using landsat time series," *Remote Sens. Environ.*, vol. 194, pp. 303–321, 2017.
[21] G. Ceccherini et al., "Abrupt increase in harvested forest area over Europe after 2015," *Nature*, vol. 583, no. 7814, pp. 72–77, 2020.
[22] N. Picard et al., "Recent increase in european forest harvests as based on area estimates (ceccherini et al. 2020a) not confirmed in the French case," *Ann. Forest Sci.*, vol. 78, pp. 1–5, 2021.
[23] A. Bouvet, S. Mermoz, M. Ballére, T. Koleck, and T. L. Toan, "Use of the SAR shadowing effect for deforestation detection with sentinel-1 time series," *Remote Sens.*, vol. 10, no. 8, 2018, Art. no. 1250.
[24] Y. Bastien, *Vocabulaire Forestier: Écologie, Gestion Et Conservation Des Espaces Boisés*. France: Forêt Privée Française, 2011.
[25] IGN, "Inventaire forestier national français, données brutes, campagnes annuelles 2005 et suivantes," 2023, Accessed: Jul. 15, 2023. [Online]. Available: https://inventaire-forestier.ign.fr/dataIFN/
[26] IGN, "Les forêts plantées en France, état des lieux," 2023, Accessed: Nov. 14, 2023. [Online]. Available: https://inventaire-forestier.ign.fr/IMG/pdf/if40_plantations.pdf
[27] T. Koleck, M. Ballère, and M. M. Sainte, "S1tiling, a multipurpose open source processing chain for Sentinel-1 time series," in *Proc. Living Planet*, 2019, pp. 13–17.
[28] S. Quegan and J. J. Yu, "Filtering of multichannel SAR images," *IEEE Trans. Geosci. Remote Sens.*, vol. 39, no. 11, pp. 2373–2379, Nov. 2001.
[29] C. Senf and R. Seidl, "Mapping the forest disturbance regimes of Europe," *Nature Sustainability*, vol. 4, no. 1, pp. 63–70, 2021.
[30] F. Mouret, D. Morin, H. Martin, M. Planells, and C. V.-Barbaroux, "Toward an operational monitoring of oak dieback with multispectral satellite time series: A case study in centre-val de loire region of France," *IEEE J. Sel. Topics Appl. Earth Observ. Remote Sens.*, vol. 17, pp. 643–659, 2024.
[31] H. Abdullah, A. K. Skidmore, R. Darvishzadeh, and M. Heurich, "Sentinel-2 accurately maps green-attack stage of European spruce bark beetle (Ips typographus, L.) compared with Landsat-8," *Remote Sens. Ecol. Conservation*, vol. 5, no. 1, pp. 87–106, Mar. 2019. [Online]. Available: https://onlinelibrary.wiley.com/doi/abs/10.1002/rse2.93
[32] L. Huo, H. J. Persson, and E. Lindberg, "Early detection of forest stress from European spruce bark beetle attack, and a new vegetation index: Normalized distance red & SWIR (NDRS)," *Remote Sens. Environ.*, vol. 255, Mar. 2021, Art. no. 112240. [Online]. Available: https://linkinghub.elsevier.com/retrieve/pii/S0034425720306131
[33] P. Stych, J. Lastovicka, R. Hladky, and D. Paluba, "Evaluation of the influence of disturbances on forest vegetation using the time series of landsat data: A comparison study of the low tatras and sumava national parks," *ISPRS Int. J. Geo- Inf.*, vol. 8, no. 2, Jan. 2019, Art. no. 71. [Online]. Available: http://www.mdpi.com/2220-9964/8/2/71
[34] D. Morin, M. Planells, S. Mermoz, and F. Mouret, "Estimation of forest height and biomass from open-access multi-sensor satellite imagery and GEDI lidar data: High-resolution maps of metropolitan France," Sep. 2023. [Online]. Available: https://hal.science/hal-04249151
[35] M. A. Tanase, C. Aponte, S. Mermoz, A. Bouvet, T. L. Toan, and M. Heurich, "Detection of windthrows and insect outbreaks by l-band SAR: A case study in the Bavarian forest national park," *Remote Sens. Environ.*, vol. 209, pp. 700–711, 2018.
[36] G. Landmann et al., "Coupes rases et renouvellement des peuplements forestiers en contexte de changement climatique," *Expertise Collective CRREF*, 2023, Art. no. 128.
[37] N. C. Coops, P. Tompalski, T. R. Goodbody, A. Achim, and C. Mulverhill, "Framework for near real-time forest inventory using multi source remote sensing data," *Forestry*, vol. 96, no. 1, pp. 1–19, 2023.
[38] C. Senf, R. Seidl, and P. Hostert, "Remote sensing of forest insect disturbances: Current state and future directions," *Int. J. Appl. Earth Observ. Geoinf.*, vol. 60, pp. 49–60, 2017.
[39] D. Marinelli, M. Dalponte, L. Frizzera, E. Næsset, and D. Gianelle, "A method for continuous sub-annual mapping of forest disturbances using optical time series," *Remote Sens. Environ.*, vol. 299, 2023, Art. no. 113852.
[40] L. Dutrieux et al., "JRC expert meeting on remote sensing-based bark beetle outbreak detection and mapping," 2023. [Online]. Available: publications.jrc.ec.europa.eu

Stéphane Mermoz received the joint Ph.D. degree, with a thesis on remote sensing of river ice in Canada using polarimetric radar data, from the National Institute of Scientific Research, Quebec City, QC, Canada, and the University of Rennes 1, Rennes, France, in 2010.

He was a Postdoctoral Researcher with the Center for the Study of the Biosphere from Space (CESBIO) till 2018, in the frame of supporting activities for the Biomass mission. He founded the GlobEO company in 2018. He is currently working on the development of methodologies to monitor forest and agriculture using remote sensing data. He participated in more than 25 projects mainly funded by ESA, CNES, and the European Commission. He has authored or coauthored more than 30 scientific papers in peer-reviewed journals. His research interests include forest aboveground biomass estimation and forest loss detection using radar data.

Dr. Mermoz was the recipient of the Postdoctoral Grant from the National Centre for Space Studies (CNES) to carry out research works in 2011. He is also a regular Reviewer of Horizon Europe projects on behalf of the European Commission.

Juan Doblas Prieto received the M.Sc. degree in geophysics from the National School of Petroleum and Motors, Paris, France, in 1997, the first postgraduation degree in environmental sciences from NADC, Universidade Federal do Rio de Janeiro, Rio de Janeiro, Brazil, in 2005, the second postgraduation degree in geographic information systems from Penn State University, Camp Hill, PA, USA, in 2010, and the Ph.D. degree in remote sensing from the Brazilian National Institute for Space Research, São Paulo, Brazil, in 2022.

He was a Mining Engineer, specialized in geology and geophysics, with the Universidad Politécnica, Madrid, Spain, in 1996. He is currently a Senior Researcher with the technology company GlobEO, associated with the National Center for Space Studies (CNES), Toulouse, France. He coordinated monitoring and territorial protection actions against deforestation in the Xingu program of the Socio-Environmental Institute (ISA). He is experienced in processing optical and SAR satellite images for detecting changes in forest cover, characterizing pressure vectors and threats to protected areas, and training in territorial mapping and monitoring techniques. After completing his doctorate, he coordinated the SAD-Cerrado initiative (IPAM/Mapbiomas). His research focuses on developing algorithms for real-time detection of changes in global forest cover.

Milena Planells received the double Engineering degrees in signal processing and satellite communications from Tlcom Paris, Paris, France, and Télécom BCN, Barcelona, Spain, in 2000, and the Ph.D. degree in modelling decoder output errors in a satellite transmission chain from Télécom Paris (Ecole Nationale Supérieur des Télécommunications), in 2003.

In 2004, she joined the French Space Agency CNES, and has been working on research and development of different space missions related to communications and Earth observation (ATHENAFIDUS, ARGOS, SARSAT, CFOSAT, and BIOMASS). She is currently a remote sensing Engineer with CESBIO Laboratory (UMR 5126), Toulouse, France. Her research focuses on crops and forest parameters retrieval and monitoring using multimodal satellite data (lidar, optical, and radar).

David Morin received the M.Sc. degree in remote sensing and environmental mapping from the University of Toulouse, Toulouse, France, in 2012, and the Ph.D. degree in environmental sciences from the SDU2E Doctoral School, University of Toulouse, Toulouse, in 2020.

From 2013 to 2016, he was an Engineer with the CESBIO Laboratory, Toulouse, France. From 2020 to 2024, he was a Postdoctoral Researcher first with CESBIO, Toulouse, France, and then with the University of Orléans, Orléans, France. He is currently a Research and Development Engineer with TerraNIS, Toulouse. His research interests include radar and optical signal processing, machine learning, and statistical analysis with remote sensing data for land use classification and vegetation monitoring.

Thierry Koleck received the Ph.D. degree in electrical engineering from Université-Paris-Sud., in 1998.

He is currently an Engineer and Researcher with CNES and CESBIO, Toulouse, France, focusing on biomass estimation and deforestation mapping using remote sensing. He has been instrumental in numerous research projects. His work leverages cutting-edge remote sensing technologies to enhance the precision of biomass estimation, which is crucial for ecological monitoring and climate change studies. His research focuses on developing advanced methodologies for accurate forest biomass assessment using satellite imagery.

Florian Mouret received the Ingénieur degree in electrical engineering and signal processing from the Ecole Nationale Supérieure d'Electronique, d'Electrotechnique, d'Informatique, d'Hydraulique et des Télécommunications de Toulouse, Toulouse, France, in 2016, and the Ph.D. degree in computer science from the National Polytechnic Institute of Toulouse, Toulouse, in 2022.

His Ph.D. thesis was carried out at the IRIT Laboratory in collaboration with TerraNIS, Toulouse. He is currently a Postdoctoral Researcher with the University of Orléans, Orléans, France, in collaboration with CESBIO Laboratory, Toulouse. His research interests include outlier detection, missing data reconstruction, and machine learning applied to remote sensing for vegetation monitoring (crops, forests).

Alexandre Bouvet received the Engineering degree in space telecommunications from the Ecole Nationale Supérieure d'Aéronautique et de l'Espace, Toulouse, France, in 2004, and the Ph.D. degree in remote sensing from the Centre d'Etudes Spatiales de la Biosphère, Université Paul Sabatier–Toulouse III, Toulouse, in 2009.

From 2010 to 2012, he was a Postdoctoral Fellow with the European Commission Joint Research Center, ISPRA, Italy, where he worked on the use of SAR data for the mapping of the African vegetation. Since 2013, he has been a Research Scientist with CESBIO, Toulouse. His research interests include SAR image processing and the use of remote sensing data to monitor vegetated areas for environmental applications (rice fields monitoring and woodlands biomass retrieval).

Thuy Le Toan received the Ph.D. degree in atomic and nuclear physics from the University of Toulouse, Toulouse, France, in 1973.

She is currently a Senior Researcher with the Centre d'Etudes Spatiales de la Biosphère (CESBIO), Toulouse, the P.I. of the BIOMASS mission, and the Co-Chair of the ESA BIOMASS Mission Advisory Group. Her research interests include microwave remote sensing for land applications, including experimental and modeling studies and SAR image analysis, with a focus on forest and agriculture, and the use of SAR data to monitor changes in the land surfaces under climatic and human impacts.

David Sheeren received the B.Sc. degree in geomatics and land surveying from the University of Liège, Liège, Belgium, in 1999, the M.Sc. degree in GIsciences from the French Engineering School of Geomatics, ENSG, Paris, France, in 2001, and the Ph.D. degree in computer science (AI) from the University Paris 6, Paris, in 2005.

From 2005 to 2006, he was a Postdoctoral Fellow with the CNRS/University of Strasbourg (ICube Lab. and LIVE Lab.). Since 2006, he has been an Associate Professor in GIsciences and remote sensing with INP-ENSAT (Engineering Faculty of Life Sciences), Toulouse, and joined the interdisciplinary research unit DYNAFOR (INRAE), Auzeville-Tolosane, France. He is also motivated by advanced methods of machine learning and their application in habitat mapping and biodiversity monitoring with Earth observation data. His research interests include remote sensing for landsacpe ecology and image analysis for mapping forest ecosystems and agroecological infrastructures.

Yousra Hamrouni received the engineering degree in agronomy, specializing in information and communication technology, from Institut Agro Montpellier, Montpellier, France, in 2015, the M.Sc. degree in remote sensing and spatial analysis from the University Paris-Est Marne-la-Vallée, Champs-sur-Marne, France, in 2016, and the Ph.D. degree in remote sensing from the National Polytechnic Institute of Toulouse, Toulouse, France, in 2021.

She is currently an Associate Professor in data science and remote sensing with the National Polytechnic Institute of Toulouse ENSAT and the DYNAFOR Lab (INRAe), Toulouse. Her research interests include developing innovative machine learning and deep learning approaches to address thematic issues related to agricultural and forestry environments using both recent and historical remote sensing data.

Thierry Belouard received the Biostatistics Master 2 degree from University of Montpellier II, in 1997, the Forestry engineering degree from Ecole nationale du Génie rural, des eaux et des forêts, Paris, in 1997, and the Agronomic engineering degree from Ecole nationale des ingénieurs des techniques agricoles, Dijon, in 1987.

He is a Researcher specializing in forest ecology and remote sensing. His contributions extend to various projects and collaborations, highlighting his expertise in forest monitoring. He has authored or coauthored papers published in journals, such as *Agricultural and Forest Entomology and Forest Ecology and Management*. His research focuses on tree species' effects on pest populations, forest pathogens, and carbon storage.

Éric Paillassa received the Ph.D. degree in phytopathologie from the University of Bordeaux 1, Bordeaux, France, in 1992.

Since 1992, he has been an Engineer with the Institut pour le Développement Forestier, Paris, France, working on national R&D projects involving forest experiments and tree species. Since 2008, he has been working on the adaptation of forests to climate change, and in particular on future species. Since 2018, he has been taking part in work on mapping poplar plantations in France using remote sensing. His research focuses on assessing, improving, and optimizing silvicultural practices for a sustainable and resilient forest that fulfills both a production function and ecosystem services.

Marion Carme received the M.Sc. degree in engineering, wood science and technology from ENSTIB (National School of Wood Technologies and Industries), Epinal, France, in 2021, and the M.Sc. degree in engineering and forest management from AgroParisTech/ENGREF (National School of Rural, Water and Forest Engineering), Nancy, France, in 2021. She is currently working toward the Ph.D. degree in forest renewal as a prerequisite for successful adaptation strategies to climate change: Evolution of germination climatic niches for european oaks and firs with the French National Research Institute for Agriculture, Food and the Environment (INRAE), Bordeaux University, Bordeaux, France.

From 2022 to 2023, she was an Engineer in charge of biomass and carbon data evaluation (SUFOSAT project, Satellite Forest Monitoring) with the Forestry Development Institute (IDF) within the National Center for Private Forests (CNPF), Bordeaux, France. Her Ph.D. topic focuses on the regeneration of European oaks and firs in the face of climate change. Her research interests include forest ecology and evolution, ecological modeling, and biogeography.

Michel Chartier received the BTEC Higher National Diploma in forest management from the Forest School of Meymac, Meymac, France, in 1997.

From 1997 to 2000, he was with the Research and Development Department, National Forestry Office. In 2000, he joined the Institute for Forestry Development to work on the themes of new technologies and remote sensing. He followed training courses around geomatics and remote sensing with AgroParisTech Montpellier, Montpellier, and Services géographiques Toulouse, Toulouse, France. He has coordinated and participated in several research programs on remote sensing with numerous partners.

Simon Martel received the engineering degree in forestry from AgroParisTech, Paris, France, in 2010.

He is a professional in the field of forestry and climate economics. He began his career with the National Center for Forest Ownership (CNPF), where he was a national climate and forest expert. In 2023, he joined the Institute for Climate Economics (I4CE) Paris, France, where he works on carbon certification and its role in promoting sustainable practices in the forest and agricultural sectors. His current research interests include the French Bas-Carbone certification scheme and the development of the European carbon removal certification framework. He is also involved in research and policy development to support economic incentives for carbon farming. He has also worked as a Research Engineer in forest dynamic modeling, INRAE in Bordeaux, Bordeaux, France.

Jean-Baptiste Féret received the Diploma in agricultural engineering from Montpellier SupAgro, Montpellier, France, in 2005, and the Ph.D. degree in environmental sciences from Université Pierre et Marie Curie, Paris, France, in 2009.

From 2010 to 2013, he was with the Asner Lab, Carnegie Institution for Science, Department of Global Ecology, Stanford, CA, USA. In 2014, he joined CNES at the CESBIO Laboratory, Toulouse, France, focusing on biodiversity mapping applications using future spaceborne imaging spectrometers and 3-D radiative transfer modeling. Since 2014, he has been with the National Research Institute of Agriculture and Environment (INRAE), Toulouse, working at the TETIS Research Unit, Montpellier. His research interests include optical remote sensing and radiative transfer modeling of vegetation, vegetation traits monitoring, and biodiversity mapping.